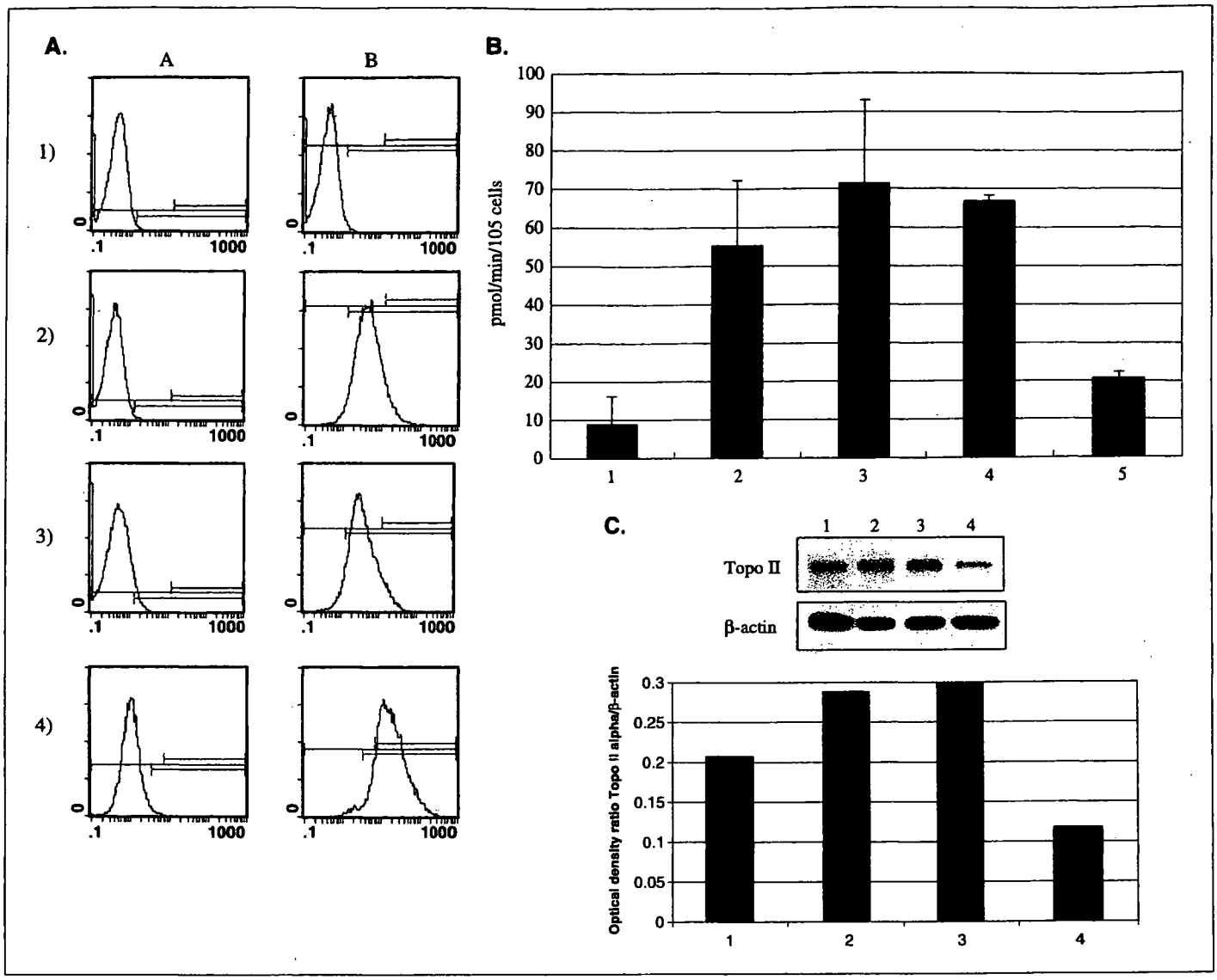

Figure 1. CD26 expression and DPPIV activity on Jiyoye-CD26 transfectants. *A*, CD26 expression on Jiyoye-CD26 transfectants. Jiyoye cells were evaluated for CD26 expression by flow cytometry as described in Materials and Methods. *1)*, Jiyoye-vector control; *2)*, Jiyoye-wtCD26-1; *3)*, Jiyoye-wtCD26-2; *4)*, Jiyoye-SACD26 transfectant (*A*, negative control; *B*, anti-CD26 antibody). Representative of three different experiments. *B*, DPPIV activity on Jiyoye-CD26 transfectants. Jiyoye cells were evaluated for DPPIV activity as described in Materials and Methods. *1)*, Jiyoye-vector control; *2)*, Jiyoye-wtCD26-1; *3)*, Jiyoye-wtCD26-2; *4)*, Jiyoye-wtCD26-3; *5)*, Jiyoye-SACD26 transfectant. *Columns*, means of three separate experiments. *C*, topoisomerase IIα expression on Jiyoye-CD26 transfectants Jiyoye cells were incubated in culture medium, and nuclear extracts were collected for immunoblotting studies to evaluate topoisomerase IIα protein levels, with β-actin as controls, as described in Materials and Methods. Each lane was equally loaded with 10 μg protein. *Lane 1*, Jiyoye-SACD26; *lane 2*, Jiyoye-wtCD26-1; *lane 3*, Jiyoye-wtCD26-2; *lane 4*, Jiyoye-vector. Representative of three different experiments.

The p38 signaling pathway is activated by various stress agents. To further characterize the effect of CD26/DPPIV on p38-mediated signaling, we stimulated Jiyoye-CD26 transfectants with UVC irradiation and phorbol 12-myristate 13-acetate (PMA). As shown in Fig. 5*A*, whereas Jiyoye-wtCD26 transfectants have greater level of baseline p38 phosphorylation than Jiyoye-vector control or Jiyoye-SACD26 transfectant, as shown above, Jiyoye-wtCD26 transfectants and Jiyoye-vector control exhibit enhanced p38 phosphorylation when stimulated with both UVC irradiation and PMA. Interestingly, Jiyoye-SACD26 transfectant displays enhanced p38 phosphorylation only when stimulated with UVC irradiation but not PMA, suggesting that different signaling events are involved for CD26/DPPIV-associated p38 phosphorylation by different stimuli. Time course studies show that PMA does not induce p38 phosphorylation in Jiyoye-SACD26 cells across the range of times tested, indicating that there is a true attenuation of phosphorylation and not merely a temporal shift in phosphorylation (Fig. 5*B*).

CD26/DPPIV Effect on Upstream Regulators of p38 in Jiyoye-CD26 Transfectants. Phosphorylation of p38 is regulated by several upstream proteins, including MKK3/MKK6. To further delineate the effect of CD26/DPPIV on p38 signaling pathway, we investigated the status of upstream regulators of p38 in Jiyoye-CD26 transfectants. Specifically, Western blot analyses with anti-phospho-MKK3/MKK6 antibody show that Jiyoye-wtCD26 transfectants have higher level of MKK3/MMK6 phosphorylation compared with Jiyoye-vector control and Jiyoye-SACD26 transfectants (Fig. 6). However, there is no detectable difference in

phosphorylation of MKK4 in these cells (data not shown), which has been described previously to contribute to p38 phosphorylation (36). We also evaluated the status of ASK1, which has a role in stress-induced apoptosis and has been found to be an upstream regulator of MKK3/MKK6 (37). Figure 6 shows that ASK1 is overexpressed in Jiyoye-wtCD26 transfectants compared with Jiyoye-vector control and Jiyoye-SACD26 cells. Interestingly, there is a higher level of phospho-ASK1 (Ser^{83}) in Jiyoye-wtCD26

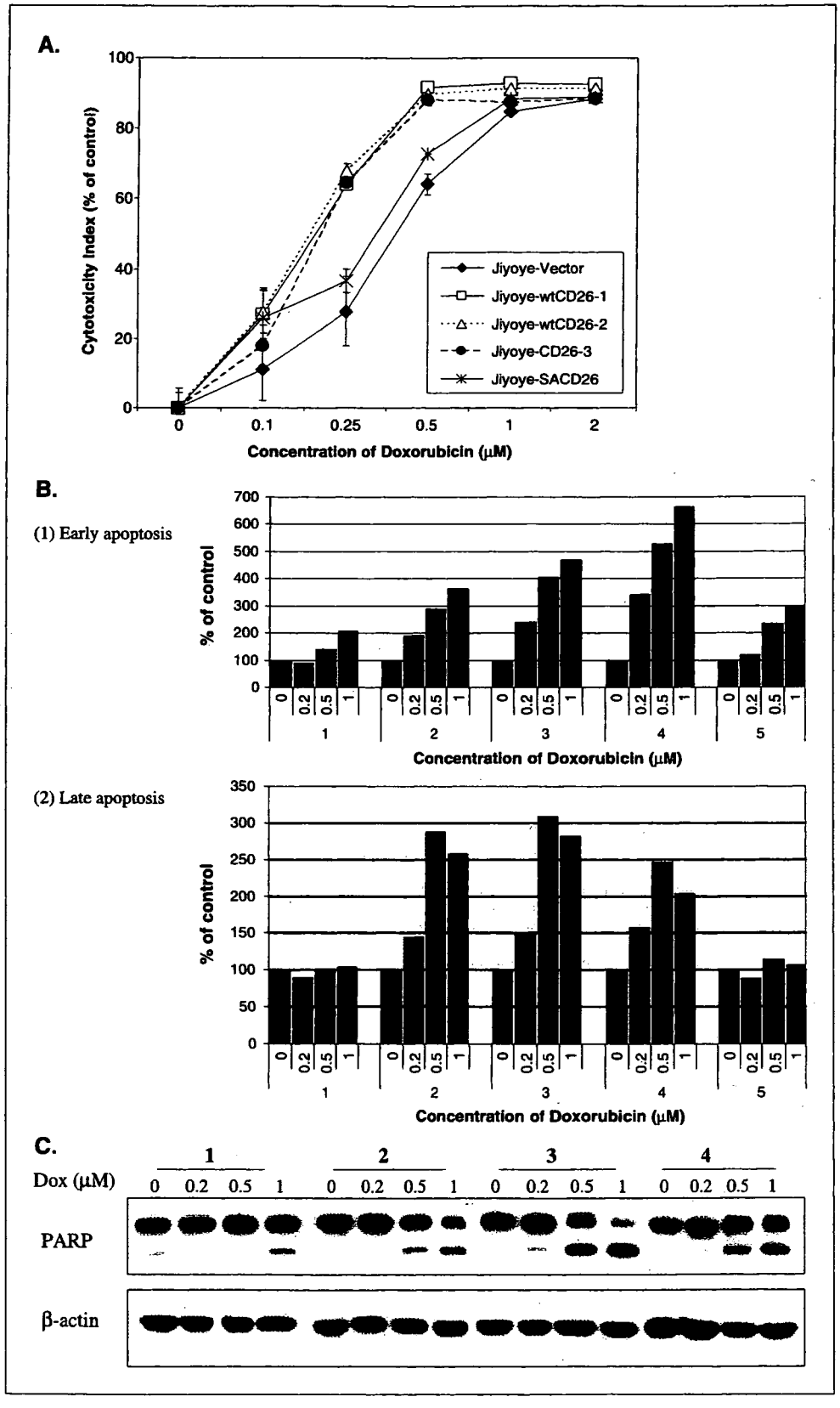

Figure 2. Effect of CD26 expression on doxorubicin-mediated growth inhibition and apoptosis. *A*, Jiyoye-CD26 transfectants were incubated at 37°C in culture medium alone or culture medium containing doxorubicin at the indicated concentrations, and 3-(4,5-dimethylthiazol-2-yl)-2, 5-diphenyltetrazolium bromide uptake assay was done as described in Materials and Methods. *Points*, means of three separate experiments. *B*, Jiyoye-vector, Jiyoye-wtCD26 transfectants, and Jiyoye-SACD26 transfectants were incubated at 37C in culture medium alone or culture medium containing doxorubicin for 48 hours at the concentrations indicated. Cells were then harvested, and Annexin V-PI assays were done as described in Materials and Methods. Cells in early stages of apoptosis were Annexin V positive, whereas Annexin V– and PI-positive cells were in late-stage apoptosis. Representative of three independent experiments. *Y axis*, % of control was calculated as follows: % of control = treated cells / nontreated cells × 100. *Group 1*, Jiyoye-vector control; *group 2*, Jiyoye-wtCD26-1; *group 3*, Jioye-wtCD26-2; *group 4*, Jiyoye-wtCD26-3; *group 5*, Jiyoye-SACD26. *C*, Jiyoye-CD26 transfectants were incubated at 37°C with medium containing doxorubicin (*Dox*) for 48 hours at the indicated doses. Cells were then harvested and whole cell lysates were obtained. Following SDS-PAGE of lysates, immunoblotting studies for poly(ADP-ribose) polymerase (*PARP*) and β-actin were done as described in Materials and Methods. The cleaved product of poly(ADP-ribose) polymerase was detected at 85 kDa. Each lane was loaded with 30 μg protein. *Group 1*, Jiyoye-vector control; *group 2*, Jiyoye-wtCD26-1; *group 3*, Jiyoye-wtCD26-2; *group 4*, Jiyoye-wtCD26-3. Representative of three different experiments.

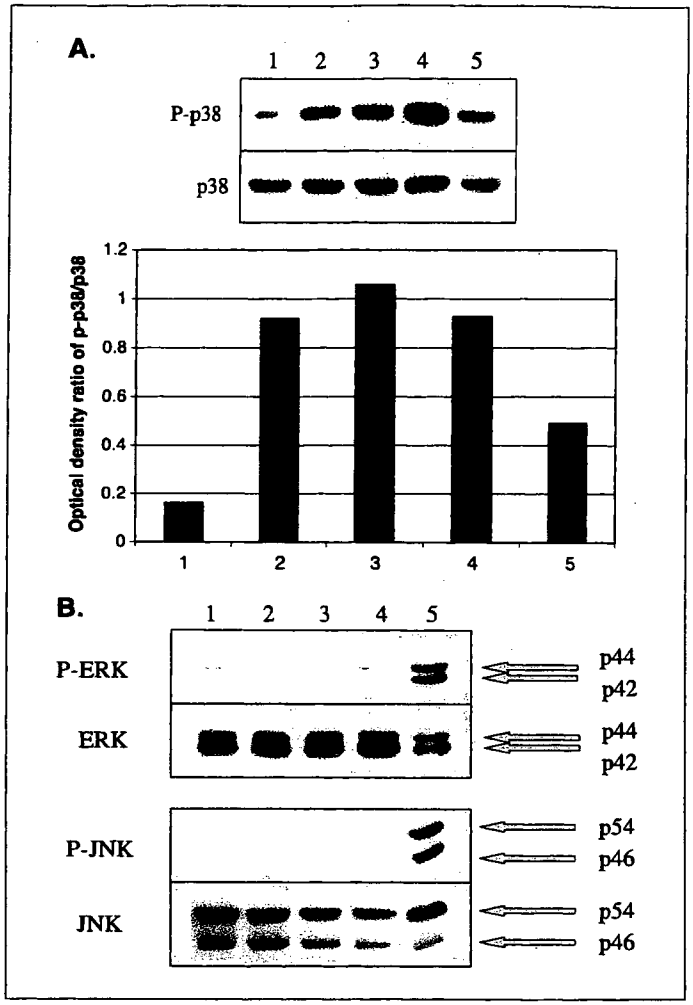

Figure 3. Increased phosphorylation of p38 on Jiyoye-CD26 transfectants. After 24 hours of incubation with culture medium, Jiyoye-vector control, Jiyoye-wtCD26 transfectants, and Jiyoye-SACD26 transfectant were harvested and whole cell lysates were obtained as described in Materials and Methods. Phosphorylation of p38, ERK, and JNK was determined with the use of phosphospecific antibodies. As positive control of phospho-ERK, parental Jiyoye cells were incubated in culture medium containing 100 nmol/L PMA for 30 minutes. As positive control of phospho-JNK, parental Jiyoye cells were washed by PBS and irradiated with UVC (254 nm: UVG-54, UVP inc. CA) for 5 minutes. After irradiation, culture media were immediately added to the cells followed by incubation for 30 minutes. Cells were then harvested and whole cell lysates were obtained with the same method as above. Each lane was loaded with 100 μg protein. *A*, p38 phosphorylation. *Lane 1*, Jiyoye-vector control; *lane 2*, Jiyoye-wtCD26-1; *lane 3*, Jiyoye-wtCD26-2; *lane 4*, Jiyoye-wtCD26-3; *lane 5*, Jiyoye-SACD26. *B*, ERK and JNK phosphorylation. *Lane 1*, Jiyoye-vector control; *lane 2*, Jiyoye-wtCD26-1; *lane 3*, Jiyoye-wtCD26-2; *lane 4*, Jiyoye-wtCD26-3; *lane 5*, positive control (*top*, ERK: PMA stimulation; *bottom*, JNK: UVC irradiation). Representative of three different experiments.

cells, whereas no significant level of phospho-ASK1 (Ser^{967}) is detected. Taken together, our findings suggest that there is an increase in the absolute number of ASK1 molecules phosphorylated at Ser^{83} in Jiyoye-wtCD26 transfectants. Meanwhile, the elevated phospho-ASK1 (Ser^{83}) level seen in conjunction with a similar increase in overall ASK1 level, along with the lack of change in phospho-ASK1 (Ser^{967}), indicates that the specific phosphate content of each ASK1 molecule is likely unchanged following CD26/DPPIV expression. Our data suggest that ASK1 and its specific phosphorylation at Ser^{83} serve as an up-regulator of CD26/DPPIV-associated p38 phosphorylation in these Jiyoye-wtCD26 transfectants.

Effect of p38 Inhibition on Topoisomerase IIα Expression. To determine the relationship between p38 phosphorylation and topoisomerase IIα expression, we evaluated topoisomerase IIα level following inhibition of p38 phosphorylation by its specific inhibitor SKF86002 (23, 38) in Jiyoye-vector controls and Jiyoye-wtCD26 transfectants. Of note is the fact that treatment with the p38 inhibitor at the indicated concentration and time course did not affect cell viability or cell cycle status (data not shown). As shown in Fig. 7, treatment with the p38 inhibitor decreases p38 phosphorylation, associated with markedly decreased topoisomerase IIα expression in both Jiyoye-vector cells and Jiyoye-wtCD26 transfectants. We found that inhibition of topoisomerase IIα expression consistently lags behind the inhibitory effect of SKF86002 on p38 phosphorylation. Whereas p38 phosphorylation is decreased from 6 to 24 hours after SKF86002 treatment, with recovery seen by 48 hours post-treatment, decreased topoisomerase IIα expression is clearly detected 48 hours post-treatment. Similar results were obtained with the p38 inhibitor SB203580 (data not shown). The fact that inhibition of p38 phosphorylation leads temporally to decreased topoisomerase IIα expression strongly suggests that p38 signaling pathway is involved in the regulation of topoisomerase IIα. Furthermore, our data show that p38-mediated regulation of topoisomerase IIα is independent of CD26 presence.

Increased Survival of Doxorubicin-Treated SCID Mice Bearing Jiyoye-wtCD26 Cells. Extending our *in vitro* findings, we investigated the effect of CD26 expression on overall survival in doxorubicin-treated SCID mice inoculated with Jiyoye-vector control or Jiyoye-wtCD26 transfectants. Jiyoye-wtCD26 transfectants or Jiyoye-vector control cells (7×10^6 cells per mouse) were implanted by i.p. injection into the SCID mice on day 0; then, once per day on days 1 and 15, animals were treated by i.p. injection with saline alone or doxorubicin at a dose of 0.5 mg/kg of body weight per injection. As shown in Fig. 8, most of the SCID mice inoculated with Jiyoye-vector control cells and treated with saline (line 1) developed tumors and then were subsequently euthanized with large tumor burden as per protocol requirements. Mice injected with Jiyoye-vector cells and treated with low-dose doxorubicin (line 2) had similar survival as those treated with saline control ($P = 0.50325$), indicating that the low-dose doxorubicin treatment did not have a statistically significant effect on tumor growth. Meanwhile, mice inoculated with Jiyoye-wtCD26 cells and treated with saline alone (line 3) exhibited in general the same survival rate as those injected with Jiyoye-vector cells and treated with saline or doxorubicin. Although there seemed to be a trend for a slight enhancement in survival among saline-treated mice inoculated with Jiyoye-wtCD26 cells (line 3) compared with Jiyoye-vector cells (line 1), the difference was not statistically significant ($P = 0.10576$). Importantly, mice inoculated with Jiyoye-wtCD26 cells and treated with doxorubicin (line 4) had a marked survival advantage compared with saline-treated mice injected with the same transfectants (line 3), which is statistically significant ($P = 0.00612$). In summary, our data show that SCID mice inoculated with Jiyoye-vector cells did not exhibit survival difference when treated with either saline or low-dose doxorubicin. However, for SCID mice inoculated with Jiyoye-wtCD26 transfectants, those treated with low-dose doxorubicin showed statistically significant difference in survival compared with those treated with saline alone. These *in vivo* results therefore extend our *in vitro* findings by demonstrating that the presence of CD26 renders tumor cells more sensitive to the antineoplastic agent doxorubicin, leading to

enhanced survival of treated animals. Our findings also suggest that treatment strategies regulating CD26 expression may be considered in the future for selected neoplasms in the clinical setting.

Discussion

In this study, we show that surface expression of CD26, especially its intrinsic DPPIV enzyme activity, results in enhanced topoisomerase IIα level in the B-cell line Jiyoye and subsequent sensitivity to doxorubicin-induced apoptosis, thus expanding our previous published work with the T-cell line Jurkat. In addition, our article is the first to show that expression of CD26/DPPIV is associated with increased p38 phosphorylation and that p38 signaling pathway plays a role in the regulation of topoisomerase IIα expression. The connection between CD26 and the p38 signaling pathway is shown in two experimental systems, one in which CD26 is overexpressed in Jiyoye transfectants and another in which CD26 expression is decreased by target-specific siRNAs in the T-cell line Karpas-299. Besides demonstrating that CD26 effect on topoisomerase IIα and doxorubicin sensitivity is applicable to cell lines of both B-cell and T-cell lineages, the potential clinical implication of our work lies with the fact that we now show for the first time that our *in vitro* findings can be extended to animal studies. Our findings that CD26 expression can be an *in vivo* marker of tumor sensitivity to doxorubicin treatment may lead to future treatment strategies targeting CD26/DPPIV for selected human cancers in the clinical setting.

MAPKs include three subfamilies: ERK, JNK/stress-activated protein kinase, and p38. Activation of the MAPK signaling pathways regulates various cellular processes, including apoptosis, proliferation, or differentiation, with the p38 signaling pathway being activated by various stress agents. In this article, we show that the presence of CD26/DPPIV results in enhanced phosphorylation of p38 in two experimental systems: the B-cell line Jiyoye in which CD26 is overexpressed and the T-cell line Karpas-299 in which CD26 expression is reduced. Previous work has shown that antibody binding to CD26 molecules expressed on the surface of CD26-Jurkat transfectants results in tyrosine phosphorylation and activation of such signaling molecules as ERK, $p56^{lck}$, $p59^{fyn}$, ZAP-70, c-Cbl, and PLC. In addition, anti-CD26 antibody-induced phosphorylation of ERK leads to expression of $p21^{Cip1}$ (26, 39). Our work is the first to clearly show that surface expression of the CD26 molecule itself is linked to increased p38 phosphorylation. Furthermore, our data suggest that upstream regulators of p38, including MKK3/MKK6 and ASK1, particularly when phosphorylated at residue Ser^{83}, is linked to the CD26/DPPIV-associated p38 signaling pathway in these Jiyoye-wtCD26 transfectants. ASK1 plays a important role in cell death induced by several stimuli, including genotoxic stress (40) and tumor necrosis factor-α (41). Meanwhile, data from Mabuchi et al. suggested that ASK1 may have a key role in determining the balance between tumor survival and apoptosis in cancer treatment (42). By affecting ASK1 phosphorylation status,

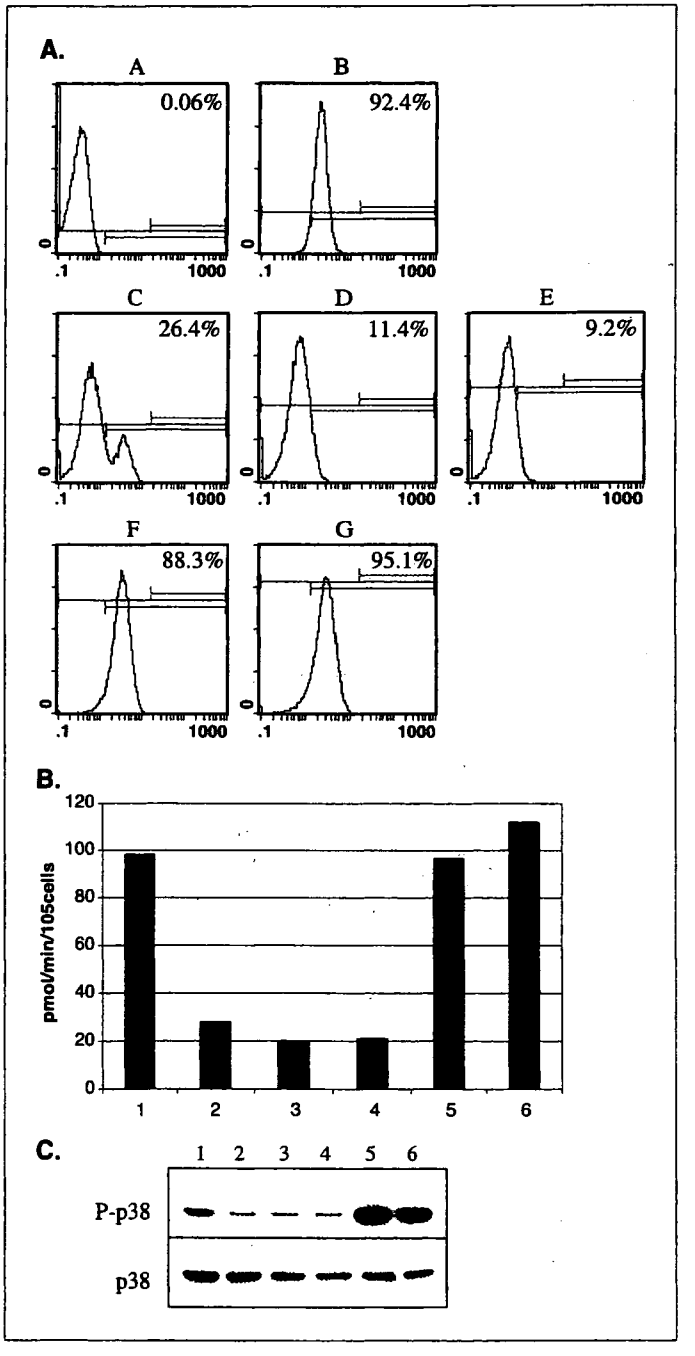

Figure 4. CD26 expression, DPPIV activity, and p38 status on Karpas-299-CD26-siRNA cells. *A*, CD26 expression on parental Karpas-299, Karpas-299-CD26-siRNA, and Karpas-299-mis-CD26-siRNA cells. Karpas-299 cells were evaluated for CD26 expression by flow cytometry as described in Materials and Methods. Amount of CD26-positive cells is presented as percentage of total cells. *A*, negative control; *B*, parental Karpas-299; *C-E*, Karpas-299-CD26-siRNA cells 1-3, respectively; *F* and *G*, Karpas-299-mis-CD26-siRNA cells 1 and 2, respectively. Representative of three different experiments. *B*, DPPIV enzyme activity on parental Karpas-299, Karpas-299-CD26-siRNA, and Karpas-299-mis-CD26-siRNA cells. Various Karpas-299 cells were evaluated for DPPIV enzyme activity as described in Materials and Methods. *Lane 1*, parental Karpas-299; *lanes 2-4*, Karpas-299-CD26-siRNA cells 1-3, respectively; *lanes 5* and *6*, Karpas-299-mis-CD26-siRNA cells 1 and 2, respectively. Representative of three different experiments. *C*, phosphorylation status of p38 on parental Karpas-299, Karpas-299-CD26-siRNA, and Karpas-299-mis-CD26-siRNA cells. After 24 hours of incubation with culture medium, parental Karpas-299 cells, Karpas-299-CD26-siRNA cells, and Karpas-299-mis-CD26-siRNA cells were harvested and whole cell lysates were obtained as described in Materials and Methods. Phosphorylation status of p38 was determined by Western blot analysis. Each lane was loaded with 100 μg protein. *Lane 1*, parental Karpas-299; *lanes 2-4*, Karpas-299-CD26-siRNA cells 1-3, respectively; *lanes 5* and *6*, Karpas-299-mis-CD26-siRNA cells 1 and 2, respectively. Representative of three different experiments.

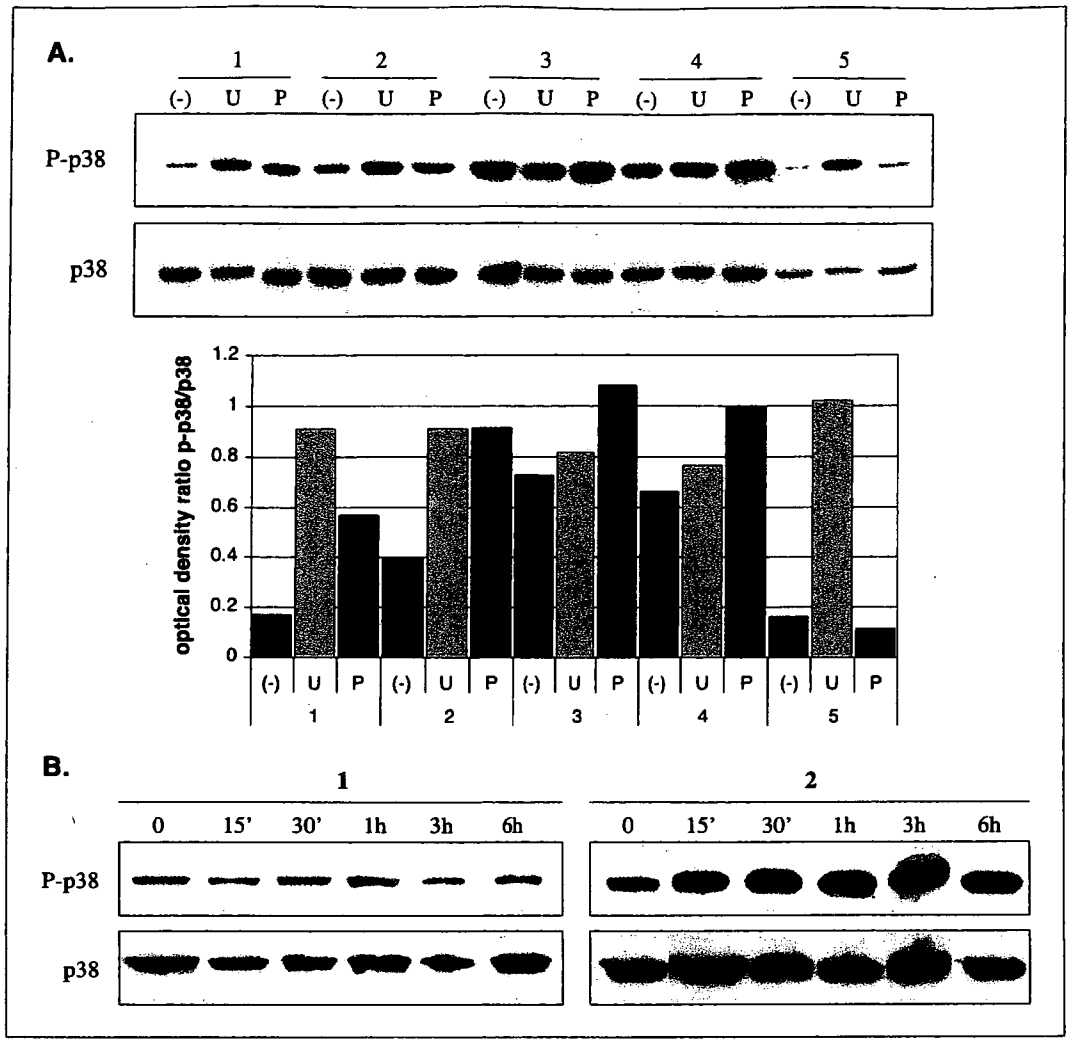

Figure 5. Effect of UVC irradiation and PMA stimulation on p38 phosphorylation in CD26 Jiyoye transfectants. *A*, After 24 hours of incubation with culture medium, Jiyoye-vector, Jiyoye-wtCD26 transfectants, and Jiyoye-SACD26 transfectant were stimulated with UVC irradiation (254 nm, 5 minutes) or PMA stimulation (100 nmol/L, 30 minutes). Cells were then harvested and whole cell lysates were obtained as described in Materials and Methods. Each lane was loaded with 100 μg protein. *(-)*, nontreatment; *U*, UVC irradiation; *P*, PMA stimulation. *Group 1*, Jiyoye-vector control; *group 2*, Jiyoye-wtCD26-1; *group 3*, Jiyoye-wtCD26-2; *group 4*, Jiyoye-wtCD26-3; *group 5*, Jiyoye-SACD26. Representative of three different experiments. *B*, cells were treated with PMA (100 nmol/L) at the indicated times, and p38 phosphorylation was detected as described above. *Group 1*, Jiyoye-SACD26; *group 2*, Jiyoye-wtCD26-1. Representative of three different experiments.

CD26/DPPIV may therefore play a potential role in key aspects of tumor biology.

Earlier work has linked constitutive p38 phosphorylation and activation to apoptosis as well as changes in cell growth status under certain experimental conditions. For example, constitutive p38 activation is associated with spontaneous apoptosis of human neutrophils; however, inhibition of p38 by its specific inhibitor and antisense RNA delays spontaneous apoptosis (43). Meanwhile, constitutive activation of p38 in B-cell tumors, including chronic lymphocytic lymphoma, diffuse large B-cell lymphoma, and follicular lymphoma, contributes to B-cell tumor growth (44). Our study links expression of CD26, particularly its DPPIV enzyme activity, to constitutive p38 phosphorylation. However, we did not detect appreciable difference in cell viability as assayed by trypan blue uptake or Annexin V-PI studies among cells differing in CD26 expression (data not shown). Whereas the presence of an intact CD26/DPPIV results in the greatest levels of p38 phosphorylation and topoisomerase IIα expression, we consistently find that Jiyoye transfectants expressing the catalytically inactive variant of CD26 still have slightly higher levels of p38 phosphorylation and topoisomerase IIα expression than Jiyoye-vector control (Figs. 1*C* and 3*A*). These findings suggest that CD26 is linked to signaling pathways independent of its peptidase activity.

Our data also show that Jiyoye cells transfected with a mutant CD26 missing the DPPIV enzyme activity (Jiyoye-SACD26 transfectant) have enhanced p38 phosphorylation only when stimulated with UVC irradiation but not when stimulated with PMA. Although the mechanisms behind this observation remain to be elucidated, several potential explanations may be considered. DPPIV activity may be associated with signaling pathways that play a role in p38 phosphorylation mediated by PMA but not by UV irradiation, and the absence of DPPIV enzyme activity may lead to the lack of engagement of these signaling pathways necessary for PMA-induced p38 phosphorylation. Regarding this point, previous work has shown that the inhibition of DPPIV enzymatic activity in T cells induces an inhibitory signaling process mainly transmitted by tyrosine kinases, resulting in the inhibition of PMA-induced $p56^{lck}$ hyperphosphorylation (45). It is also possible that phorbol esters and UV irradiation engage different downstream signals to phosphorylate p38 that are differentially associated with CD26 and its intrinsic DPIPV enzyme activity. Previous work has shown that p38 activation is differentially regulated by PMA and UV irradiation in other experimental conditions (46). Furthermore, UV irradiation induces the activation of all p38 isoforms, whereas PMA stimulation activates only the p38 γ and δ isoforms (38). Our results also show a connection between p38 and topoisomerase IIα, as inhibition of p38 phosphorylation by a specific p38 inhibitor reduces topoisomerase IIα expression. The fact that decreased topoisomerase IIα level is seen 48 hours after

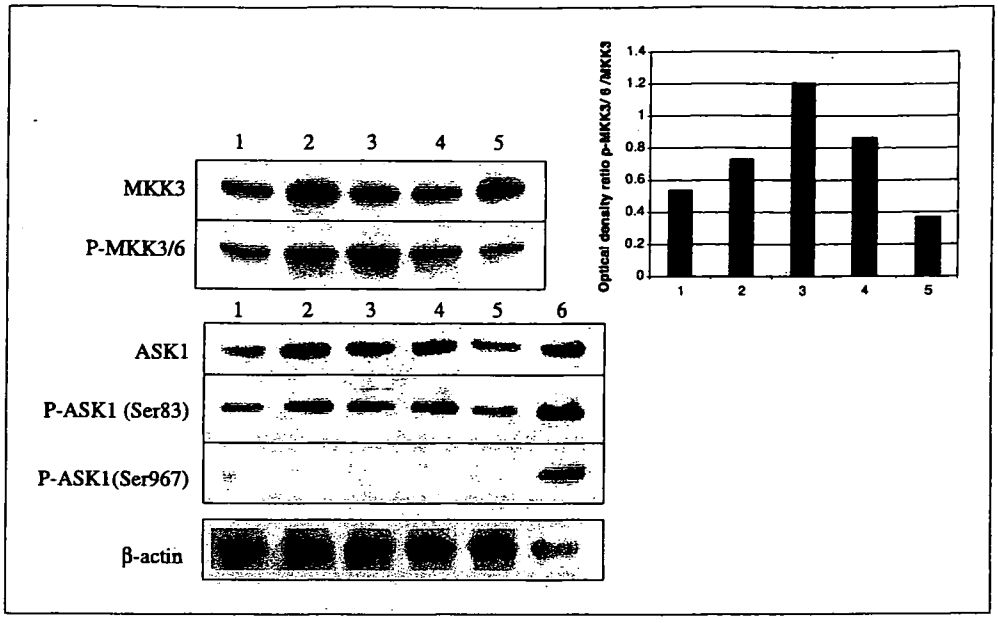

Figure 6. Constitutive p38 phosphorylation and its correlation with MKK3/MKK6 and ASK1 phosphorylation in CD26 Jiyoye transfectants. After 24 hours of incubation with culture medium, Jiyoye-Vector, Jiyoye-wtCD26 transfectants, and Jiyoye-SACD26 transfectant were harvested and whole cell lysates were obtained as described in Materials and Methods. Each lane was loaded with 100 μg protein. MKK3/MKK6 and ASK1 phosphorylation status was determined with the use of phosphospecific antibodies. For ASK1, specific antibodies can detect phosphorylation at Ser^{83} and Ser^{967}. *Lane 1,* Jiyoye-vector; *lane 2,* Jiyoye-wtCD26-1; *lane 3,* Jiyoye-wtCD26-2; *lane 4,* Jiyoye-wtCD26-3; *lane 5,* Jiyoye-SACD26; *lane 6,* UVC irradiation 5 minutes (for positive control). Representative of three different experiments.

treatment with the p38 inhibitor, whereas inhibition of p38 phosphorylation is seen earlier at 6 hours post-treatment, also suggests that p38 signaling pathway has a role in regulating topoisomerase IIα expression. The fact that p38 regulates topoisomerase IIα expression in both Jiyoye-vector controls and Jiyoye-wtCD26 transfectants indicates that this is a CD26-independent process. Furthermore, our data show that the increase in topoisomerase IIα associated with the ectopic expression of CD26 is controlled by existing p38-linked pathways regulating topoisomerase IIα expression. To our knowledge, our work is the first to show a potential connection between these two intracellular proteins, including the potential regulation of topoisomerase IIα level by p38.

Meanwhile, our data showing that the expression of CD26, especially its intrinsic DPPIV enzyme activity, is associated with enhanced topoisomerase IIα level and increased doxorubicin sensitivity in the B-cell lymphoma line Jiyoye extend our previous findings with the T-cell line Jurkat (19, 20). Whereas CD26 role in normal T-lymphocyte physiology is well established and its involvement in selected T-cell tumors is being elucidated (1, 7, 8, 47), CD26 function in B cells has not been well studied. Our work therefore suggested that CD26/DPPIV effect on topoisomerase IIα and subsequent doxorubicin sensitivity is not restricted only to tumors of T-cell lineage but is also applicable potentially to other lymphoid malignancies. Recently, topoisomerase IIα expression on malignant tumors has been found to correlate response to treatment of malignant tumors and longer patient survival, including breast cancer and Hodgkin's disease (48, 49). In addition, Walker and Nitiss show that an increase in topoisomerase IIα gene copy number is associated with cancers that have increased sensitivity to topoisomerase II inhibitors, such as doxorubicin (50). Importantly, we show for the first time that our *in vitro* results can be extended to and confirmed in animal studies. Specifically, the presence of CD26 renders tumor cells more sensitive to doxorubicin, resulting in statistically significant survival advantage. SCID mice injected with Jiyoye control cells treated with low-dose doxorubicin did not show any significant difference in survival compared with those treated with saline, whereas SCID mice inoculated with Jiyoye-wtCD26 transfectants showed significantly greater survival when treated with low-dose doxorubicin than with saline alone. Interestingly, our *in vivo*

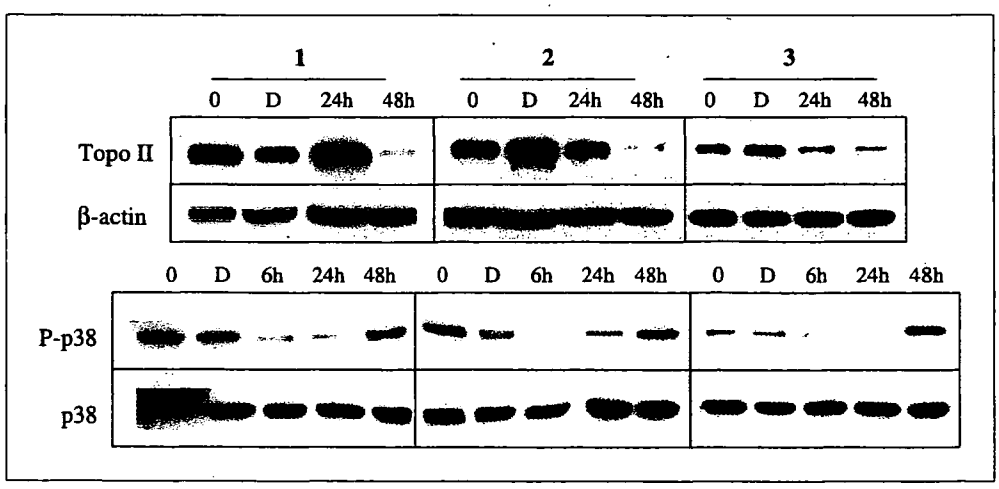

Figure 7. Effect of inhibition of p38 phosphorylation on topoisomerase IIα expression. Jiyoye-wtCD26 transfectants and Jiyoye-vector controls were incubated in culture medium alone or culture medium containing SKF86002 (20 μmol/L) for either 24 or 48 hours. Cells were then harvested and nuclear extracts were obtained. Following SDS-PAGE of lysates, immunoblotting studies for topoisomerase IIα (*Topo II*) or β-actin were done as described in Materials and Methods. Each lane was loaded with 20 μg protein. *D,* DMSO control. *Group 1,* Jiyoye-wtCD26-1; *group 2,* Jiyoye-wtCD26-2; *group 3,* Jiyoye-vector controls. At various times, an aliquot was removed and stained with trypan blue dye to evaluate cell viability with a hemocytometer. All experiments had >95% cell viability. Representative of three different experiments.

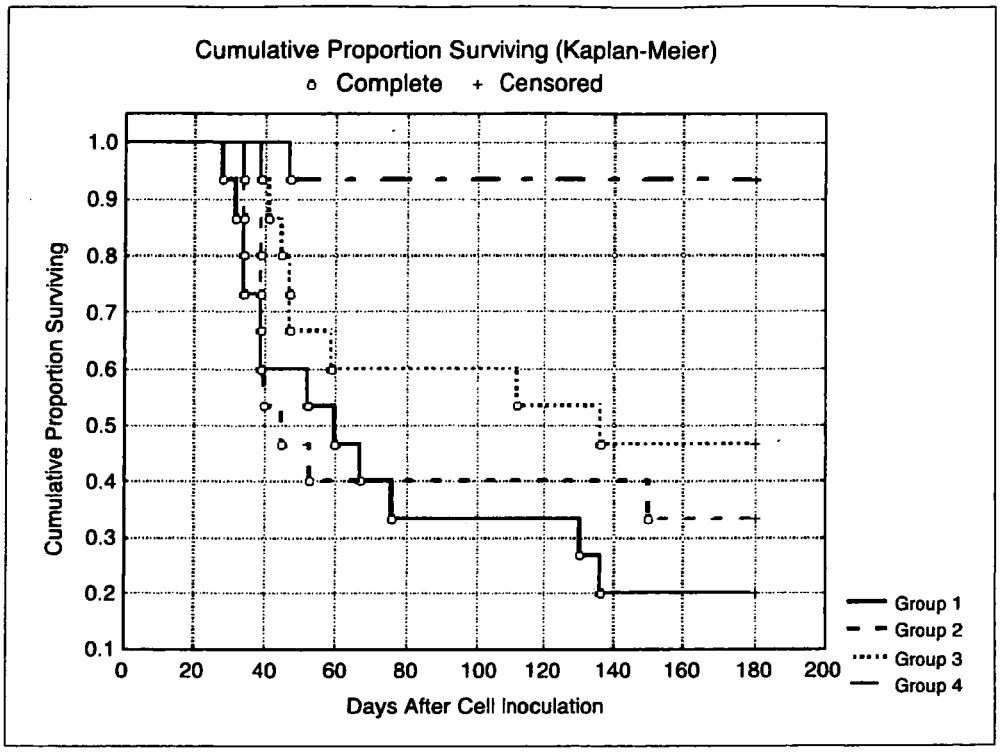

Figure 8. Enhanced survival of Jiyoye-CD26 transfectant-bearing SCID mice after doxorubicin treatment. SCID mice were injected with Jiyoye-vector control cells or Jiyoye-wtCD26-1 cells (7×10^6 cells per mouse) on day 0 and treated with saline or doxorubicin 0.5 mg/kg) on days 1 and 15 as described in Materials and Methods. Each treatment group consisted of 15 mice. *Group 1*, Jiyoye-vector control treated with saline alone; *group 2*, Jiyoye-vector control treated with doxorubicin; *group 3*, Jiyoye-wtCD26 transfectant treated with saline alone; *group 4*, Jiyoye-wtCD26 transfectant treated with doxorubicin. Analysis for statistically significant differences in survival was done using a log-rank test (*P*s: 1 versus 2 = 0.50325, 1 versus 3 = 0.10576, 1 versus 4 = 0.00009, 2 versus 3 = 0.25056, 2 versus 4 = 0.00070, and 3 versus 4 = 0.00612).

studies also suggested that the presence of CD26 itself enhances survival, although the difference in survival between the Jiyoye-wtCD26 group treated with saline alone and the Jiyoye-vector control group treated with saline alone did not reach statistical significance in our experiments. Although our studies may have been underpowered to detect this difference, this potential effect resulting from CD26 expression may indicate that CD26 presence itself can modulate tumor engraftment or tumorigenicity of the transplanted cells. Regarding this point, other groups have shown that CD26/DPPIV expression in melanoma, lung carcinoma, and ovarian carcinoma inhibits tumorigenicity and prolongs survival time (14–16). Taken together, our findings thus have potential implications in the clinical setting, suggesting that future treatment strategies that involve CD26/DPIV may be effective for selective neoplasms of both B-cell and T-cell lineages.

Acknowledgments

Received 7/21/2004; revised 11/8/2004; accepted 12/20/2004.

Grant support: M.D. Anderson Cancer Center Physician-Scientist Award, Gillson Longenbaugh Foundation, and Goodwin Funds (N.H. Dang).

The costs of publication of this article were defrayed in part by the payment of page charges. This article must therefore be hereby marked advertisement in accordance with 18 U.S.C. Section 1734 solely to indicate this fact.

References

1. Dang NH, Morimoto C. CD26: an expanding role in immune regulatilkon and cancer. Histol Histopathol 2002;17:1213–26.
2. Morimoto C, Torimoto Y, Levinson G, et al. 1F7, a novel cell surface molecule, involved in helper function of CD4 cells. J Immunol 1989;143:3430–9.
3. Ishii T, Ohnuma K, Murakami A, et al. CD26-mediated signaling for T cell activation occurs in lipid rafts through its association with CD45RO. Proc Natl Acad Sci U S A 2001;98:12138–43.
4. Ikushima H, Munakata Y, Ishii T, et al. Internalization of CD26 by mannose 6-phosphate/insulin-like growth factor II receptor contributes to T cell activation. Proc Natl Acad Sci U S A 2000;97:8439–44.
5. Kameoka J, Tanaka T, Nojima Y, Schlossman SF, Morimoto C. Direct association of adenosine deaminase with a T cell activation antigen, CD26. Science 1993;261:466–9.
6. Ohnuma K, Yamochi T, Uchiyama M, et al. CD26 up-regulates expression of CD86 on antigen-presenting cells by means of caveolin-1. Proc Natl Acad Sci U S A 2004;101:14186-91.
7. Carbone A, Gloghini A, Zagonel V, et al. The expression of CD26 and CD40L is mutually exclusive in human T-cell non-Hodgkin's lymphomas/leukemia. Blood 1995;86: 4617–26.
8. Dang NH, Aytac U, Sato K, et al. T-large granular lymphocyte lymphoproliferative disorder: expression of CD26 as a marker of clinically aggressive disease and characterization of marrow inhibition. Br J Haematol 2003;121:857–65.
9. Bauvois B, De Meester I, Dumont J, Rouillard D, Zhao HX, Bosmans E. Constitutive expression of CD26/dipeptidase IV on peripheral blood B lymphocytes of patients with B chronic lymphocytic leukemia. Br J Cancer 1999;79:1042–8.
10. Aratake Y, Kotani T, Tamura K, et al. Dipeptidyl aminopeptidase IV staining of cytologic preparations to distinguish benign and malignant thyroid diseases. Am J Clin Pathol 1991;96:306–10.
11. Bogenrieder T, Finstad CL, Freeman RH, et al. Expression and localization of aminopeptidase A, aminopeptidase N, and dipeptidyl peptidase IV in benign and malignant human prostate tissue. Prostate 1997;33:225–32.
12. Ten Kate J, van den Ingh HF, Khan PM, Bosman FT. Adenosine deaminase complexing protein (ADCP) immunoreactivity in colorectal adenocarcinoma. Int J Cancer 1986;37:479–85.
13. Morrison ME, Vijayasaradhi S, Engelstein D, Albino AP, Houghton AN. A marker for neoplastic progression of human melanocytes is a cell surface ectopeptidase. J Exp Med 1993;177:1135–43.
14. Wesley UV, Albino AP, Tiwari S, Houghton AN. A role for dipeptidyl peptidase IV in suppressing the malignant phenotype of melanocytic cells. J Exp Med 1999; 190:311–22.
15. Wesley UV, Tiwari S, Houghton AN. Role for dipeptidyl peptidase IV in tumor suppression of human non small cell lung carcinoma cells. Int J Cancer 2004; 109:855–66.
16. Kajiyama H, Kikkawa F, Suzuki T, Shibata K, Ino K, Mizutani S. Prolonged survival and decreased invasive activity attitude to dipeptidyl peptidase IV over-expression in ovarian carcinoma. Cancer Res 2002;62: 2753–7.
17. Kellner U, Sehested M, Jensen PB, Gieseler F, Rudolph P. Culprit and victim—DNA topoisomerase II. Lancet Oncol 2002;3:235–43.
18. Aytac U, Claret FX, Ho L, et al. Expression of CD26 and its associated dipeptidyl peptidase IV enzyme activity enhances sensitivity to doxorubicin-induced cell cycle arrest at the G_2-M checkpoint. Cancer Res 2001;61:7204–10.
19. Aytac U, Sato K, Yamochi T, et al. Effect of CD26/dipeptidyl peptidase IV on Jurkat sensitivity to G_2-M arrest induced by topoisomerase II inhibitors. Br J Cancer 2003;88:455–62.
20. Sato K, Aytac U, Yamochi T, et al. CD26/dipeptidyl peptidase IV enhances expression of topoisomerase IIα

and sensitivity to apoptosis induced by topoisomerase II inhibitors. Br J Cancer 2003;89:1366–74.
21. Su B, Karin M. Mitogen-activated protein kinase cascades and regulation of gene expression. Curr Opin Immunol 1996;8:402–11.
22. Platanias LC. Map kinase signaling pathways and hematologic malignancies. Blood 2003;101:4667–79.
23. Losa JH, Cobo CP, Viniegra JG, et al. Role of the p38 MAPK pathway in cisplatin-based therapy. Oncogene 2003;22:3998–4006.
24. Zhao Y, You H, Yang Y, et al. Distinctive regulation and function of PI3K/Akt and MAPKs in doxorubicin-iInduced apoptosis of human lung adenocarcinoma cells. J Cell Biochem 2004;91:621–32.
25. Kahne T, Reinhold D, Neubert K, Born I, Faust J, Ansorge S. Signal transduction events induced or affected by inhibition of the catalytic activity of dipeptidyl peptidase IV (DPIV, CD26). Adv Exp Med Biol 2000;477:131–7.
26. Ohnuma K, Ishii T, Iwata S, et al. G_1-S cycle arrest provoked in human T cells by antibody to CD26. Immunology 2002;107:325–33.
27. Tanaka T, Camerini D, Seed B, et al. Cloning and functional expression of the T cell activation antigen CD26. J Immunol 1992;149:481–6.
28. Gum JR, Erickson RH, Hicks JW, Rius JL, Kim YS. Analysis of dipeptidyl peptidase IV gene regulation in transgenic mice: DNA elements sufficient for promoter activity in the kidney, but not the intestine, reside on the proximal portion of the gene 5′-flanking region. FEBS Lett 2000;482:49–53.
29. Reikofski J, Tao BY. Polymerase chain reaction (PCR) techniques for site-directed mutagenesis. Biotechnol Adv 1992;10:535–47.
30. Tanaka T, Kameoka J, Yaron A, Schlossman SF, Morimoto C. The costimulatory activity of the CD26 antigen requires dipeptidyl peptidase IV enzyme activity. Proc Natl Acad Sci U S A 1993;90:4586–90.
31. Hansen MB, Nielsen SE, Berg K. Re-examination and further development of a precise and rapid dye method for measuring cell growth/cell kill. J Immunol Methods 1989;119:203–10.
32. Dang NH, Torimoto Y, Sugita K, et al. Cell surface modulation of CD26 by anti-1F7 monoclonal antibody; analysis of surface expression and human T cell activation. J Immunol 1990;145:3963–71.
33. Raynal P, Pollard HB. Annexins: the problem of assessing the biological role for a gene family of multifunctional calcium- and phospholipids-binding proteins. Biochem Biophys Acta 1994;1197:63–93.
34. Roulston A, Reinhard C, Amiri P, Williams LT. Early activation of c-Jun N-terminal kinase and p38 kinase regulate cell survival in response to tumor necrosis factor α. J Biol Chem 1998;273:10232–9.
35. Ho L, Aytac U, Stephens C, et al. *In vitro* and *In vivo* antitumor effect of the anti-CD26 monoclonal antibody 1F7 on human CD30$^+$ anaplastic large cell T-cell lymphoma Karpas 299. Clin Cancer Res 2001;7:2031–40.
36. Derijard B, Raingeaud J, Barrett T, et al. Independent human MAP-kinase signal transduction pathways defined by MEK and MKK isoforms. Science 1995;267:682–5.
37. Ichijo H, Nishida E, Irie K, et al. Induction of Apoptosis by ASK1, a Mammalian MAPKKK that activates SAPK/JNK and p38 signaling pathways. Science 1997;275:90–4.
38. Kumar S, McDonnell PC, Gum RJ, Hand AT, Lee JC, Young PR. Novel homologues of CSBP/p38 MAP kinase: activation, substrate specificity and sensitivity to inhibition by pyridinyl imidazoles. Biochem Biophys Res Commun 1997;235:533–8.
39. Hegen M, Kameoka J, Dong RP, Schlossman SF, Morimoto C. Cross-linking of CD26 by antibody induces tyrosine phosphorylation and activation of mitogen-activated protein kinase. Immunology 1997; 90:257–64.
40. Wang TH, Wang HS, Ichijo H, et al. Microtubule-interfering agents active c-Jun N-terminal kinase/stress-activated protein kinase through both Ras and apoptosis signal-regulating kinase pathways. J Biol Chem 1998;273:4928–36.
41. Chen Z, Seimiya H, Naito M, et al. ASK1 mediates apoptotic cell death induced by genotoxic stress. Oncogene 1999;18:173–80.
42. Mabuchi S, Ohmichi M, Kimura A, et al. Estrogen inhibits paclitaxel-induced apoptosis via the phosphorylation of apoptosis signal-regulating kinase 1 in human ovarian cancer cell lines. Endocrinology 2004;145:49–58.
43. Aoshiba K, Yasui S, Hayashi M, Tamaoki J, Nagai A. Role of p38-mitogen-activated protein kinase in spontaneous apoptosis of human neutrophils. J Immunol 1999;162:1692–700.
44. Ogasawara T, Yasuyama M, Kawauchi K. Constitutive activation of extracellular signal-regulated kinase and p38 mitogen-activated protein kinase in B-cell lymphoproliferative disorders. Int J Hematol 2003;77:364–70.
45. Kahne T, Neubert K, Faust J, Ansorge S. Early phosphorylation events induced by DPIV/CD26-specific inhibitors. Cell Immunol 1998;189:60–6.
46. Raingeaud J, Gupta S, Rogers JS, et al. Pro-inflammatory cytokines and environmental stress cause p38 mitogen-activated protein kinase activation by dual phosphorylation on tyrosine and threonine. J Biol Chem 1995;270:7420–6.
47. Sato K, Dang NH. CD26: a novel treatment target for T-cell lymphoid malignancies? Int J Oncol 2003;22: 481–97.
48. Jarvinen TA, Liu ET. HER-2/*neu* and topoisomerase IIα in breast cancer. Breast Cancer Res Treat 2003; 78:299–311.
49. Provencio M, Corbacho C, Salas C, et al. The topoisomerase IIa expression correlates with survival in patients with advanced Hodgkin's lymphoma. Clin Cancer Res 2003;9:1406–11.

Clinical and Experimental Immunology EDITORIAL REVIEW doi:10.1111/j.1365-2249.2005.02683.x

CD26$^+$ T cells in the pathogenesis of asthma

K. Ohnuma,* T. Yamochi,* O. Hosono* and C. Morimoto*

**Division of Clinical Immunology, Advanced Clinical Research Centre, Institute of Medical Science, University of Tokyo, Tokyo, Japan*

Keywords: CD26, dipeptidyl peptidase IV, asthma, chronic inflammation, T cell

Accepted for publication 26 October 2004

Correspondence: Dr. C. Morimoto, Division of Clinical Immunology, Advanced Clinical Research Centre, Institute of Medical Science, University of Tokyo, 4-6-1, Shirokanedai, Minato-ku, Tokyo 108-8639, Japan.
E-mail: morimoto@ims.u-tokyo.ac.jp

Asthma is a chronic inflammatory disease of the small airways, being clinically characterized by reversible airway obstruction and bronchial hyperreactivity [1]. These clinical features result from a chronic inflammation of the airways, caused by a migration of leucocytes and an increase of inflammatory mediators in the bronchial wall [2]. This pathological reaction in asthma is thought to arise from a complex interaction between genes and the environment.

Although allergens and infection appear to be environmental modifiers of asthma [3,4], it is now estimated that at least a dozen polymorphic genes regulate asthma and control the chronic inflammatory response and production of immunoglobulin E (IgE), cytokines and chemokines. By genetic-linkage analysis on 460 pairs of siblings from asthmatic families in the USA and UK, Van Eerdewegh *et al.* [5] identified a locus on the short arm of chromosome 20 which was linked to asthma and bronchial hyperreactivity. They identified the *ADAM-33* gene as significantly associated with asthma. ADAMs are a subfamily of metalloproteinases expressed on the cell surface, and have proteolytic functions such as shedding tumour necrosis factor receptors, and other cell-surface cytokines, adhesion molecules, and growth factors and receptors that are involved in inflammation, cell proliferation, and cell death. *ADAM-33* is expressed by lung fibroblasts and bronchial smooth muscle cells, and is suspected to be associated with small-airway remodeling in patients with asthma.

Regarding immunological aspects of asthma genes, the human homologue of *Tim1* has been identified as an asthma susceptibility gene [6]. *Tim1* lies at chromosome 5q33.2, a region that has been repeatedly linked to asthma, and codes for the cellular receptor for hepatitis A virus [6]. The *Tim1* gene product is expressed on T cells and appears to regulate the production of interleukin-4 (IL-4) in T cells by affecting CD4+ T cell differentiation, the development of T_H2 cells and development of airway hyperreactivity. As observed in the *Tim1* hypothesis, the inappropriate T_H2 response causes pulmonary inflammation, airway eosinophilia, and airway hyperreactivity to a variety of specific and nonspecific stimuli that result in the clinical symptoms of asthma.

In the T_H1-T_H2 paradigm, T_H1 cell responses are thought to protect against asthma, by dampening the activity of T_H2 responses [7–9]. However, other investigators have shown that T_H1 cells may exacerbate asthma, as human asthma is associated with the production of IFN-γ which appears to contribute to pathogenesis of asthma [10,11]. Allergen-specific T_H1 cells, when adoptively transferred into naïve recipients, migrate to the lungs but fail to counterbalance T_H2 cell-induced airway hyperreactivity. Instead, allergen-specific T_H1 cells cause severe airway inflammation [12]. Moreover, Dahl *et al.* [13] showed virus-induced T_H1-dependent enhancement of allergic pulmonary inflammation via T_H1-polarized dendritic cells (DCs). Thus, although T_H2 cells play an important role in the pathogenesis of asthma, the binary T_H1-T_H2 paradigm cannot explain all the immunological processes that occur in asthma. These processes in asthma may be much more complex than is hypothesized by a T_H1-T_H2 paradigm. In this regard, Kruschinski *et al.* [14], in this issue of *Clinical and Experimental Immunology*, show a critical role for CD26$^+$ T cells, which are T_H1 cells, in asthma, by examining CD26-deficient and CD26-reduced rats in ovalubmin (OVA)-induced asthma models. They show in their article that the decrease in T cell recruitment to the airway observed in CD26^{low} and CD26-deficient rats is associated with significantly reduced OVA-specific IgE-titres. They suggest a role for CD26$^+$ T cells in the pathogenesis of asthma by means of T cell migration and T cell-dependent IgE production in the airway.

CD26/dipeptidyl peptidase IV (DPPIV) is a 110-kDa cell surface glycoprotein that belongs to the serine protease

family [15]. It is expressed on a variety of tissues including T lymphocytes, endothelial and epithelial cells. It is composed of a short cytoplasmic domain of 6 amino acids, a transmembrane region of 22 amino acids, and an extracellular domain of 738 amino acids, with DPPIV activity which selectively removes the N-terminal dipeptide from peptides with proline or alanine in the second position [16]. Possible substrates of DPPIV include several critical cytokines and chemokines. Activity of CCL5 (RANTES, regulated on activation, normal T cell expressed and secreted) is altered by the enzymatic cleavage of DPPIV, as CD26-processed CCL5(3–68) has a more than 10 times lower chemotactic potency for monocytes and eosinophils. CCL5(3–68) also has impaired binding and signalling properties through CCR1 and CCR3, but remains fully active on CCR5, leading to T_H1 polarization [17,18]. Other important chemokines that appear to be substrates of the enzymatic activity of DPPIV include CCL11 (eotaxin), CCL22 (macrophage-derived chemokine), CXCL10 and CXCL11 (interferon inducible chemokines), and other chemokines [19,20]. Besides its ability to regulate the effect of biological factors through its enzymatic activity, CD26/DPPIV has an essential role in human T cell physiology.

Originally characterized as a T-cell differentiation antigen, CD26 is preferentially expressed on a specific population of T lymphocytes, the subset of CD4+ memory T cells, and is up-regulated after T cell activation [21,22]. As well as its enhanced expression on activated T cells, various lines of evidence have converged to demonstrate that CD26 is functionally associated with T cell signal transduction processes, which are capable of transmitting signals relating to T cell activation [22,23]. In addition CD26 serves as a functional collagen receptor with a role in T cell activation, as well as having a potential role in thymic ontogeny [24]. The enzymatic activity of CD26 appears to be very important in enhancing cellular responses to external stimuli. For example, Jurkat cells transfected with wild type CD26 consistently demonstrated greater activation than parental CD26 nega-

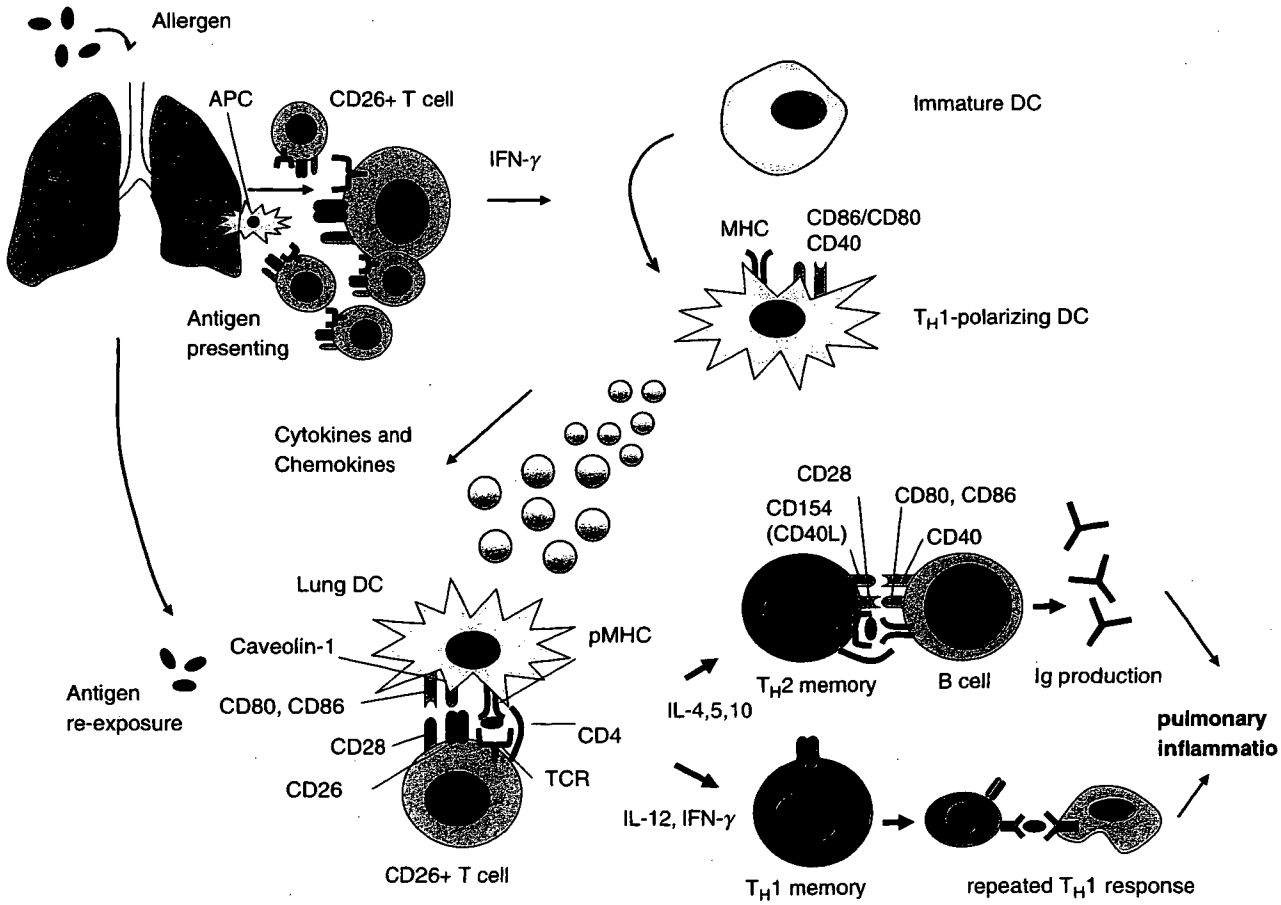

Fig. 1. T_H1-dependent enhancement of allergic pulmonary inflammation. Initially, antigens such as sensitizing-allergens stimulate $CD26^+$ T cells via antigen presenting cells (APC), and subsequently generate $CD26^+$ T_H1 response to produce IFN-γ and stable T_H1-polarizing DCs. Later, these DCs are capable of augmenting both T_H1 and T_H2 controlled immune responses in allergen-induced pulmonary inflammation, partly via interaction of CD26 on T cells and caveolin-1 on APC loaded with sensitized allergens. Ig, immunoglobulin; MHC, major histocompatibility complex; pMHC, peptide-loaded major histocompatibility complex.

tive Jurkat or cells transfected with CD26 mutated at the DPPIV enzymatic site [25].

CD26 expression is tightly regulated on human T lymphocytes, with its density being markedly elevated following T cell activation [21,26]. At the resting state in the peripheral blood, CD26 is preferentially expressed on the helper/memory T cell population [21]. High CD26 cell surface expression is correlated with the production of T_H1-like cytokines by T-cell clones, and CD26 expression is induced by stimuli that favour the development of the T_H 1 response [27,28]. CD26 is able to conduct IL-2-dependent comitogenic signals in conjunction with activation through the CD3/T cell receptor complex or the CD2 pathway of mature human T lymphocytes when crosslinked with solid-phase immobilized antibodies [22].

Meanwhile, recombinant soluble CD26/DPPIV molecule up-regulates expression of CD86 on antigen presenting cells (APC), leading to greater APC–T cell interaction and enhanced T cell proliferation, with important implications for immunoregulation [29]. More recently, T cell proliferation via CD26 driven by recall antigens such as tetanus toxoid is mediated by means of caveolin-1 on APC, leading to up-regulation of the costimulatory molecule CD86 [30]. Thus, CD26+ T cells play a critical role in inflammation responding to recall antigen.

Of clinical relevance, patients with autoimmune diseases such as Graves' disease and rheumatoid arthritis have been found to increase numbers of CD26+ T cells in inflamed tissues such as thyroid and synovial fluids [26,31]. In addition, enhancement of CD26 expression in these autoimmune diseases may correlate with disease severity [32,33]. Moreover, we have shown that T cells migrating through endothelial cell monolayers *in vitro* express high levels of CD26 [34], and the fact that chemokines play a key role in T cell migration supports the notion that CD26/DPPIV may interact with chemokines [18–20]. These findings imply that CD26+ T cells play a role in the inflammation process and subsequent tissue damage not only in autoimmune diseases, but also in asthma.

In the context that CD26+ T cells preferentially play an important role in allergic pulmonary inflammation, it is hypothesized that allergens such as OVA incite a robust T_H1-type cytokine response, such as IFN-γ, in the lung, promoting the development of durable T_H1-polarizing DCs, partly via a CD26–caveolin-1 interaction, subsequently leading to enhancement of CD28-CD86 costimulation (Fig. 1). These DCs support subsequent immunity in a T_H2-dependent process of allergen-induced pulmonary inflammation, and so enhance both T_H1 and T_H2 immune cytokines and IgE production.

Interestingly, a recent report on single-nucleotide polymorphism in asthmatic patients revealed that polymorphism of DPP-10, a CD26/DPPIV-like peptidase, was observed [35]. Further elucidation on DPPs and asthma will open an avenue for our understanding the pathophysiology of asthma.

Although the precise effects rely on the exact timing, intensity and dose of cytokines and antigens as well as how these interactions alter T helper regulatory cells and cytokines, CD26+ T cells play an important role in asthma and targeting CD26/DPPIV may contribute to the elucidation of the pathophysiology and therapeutic means to treat asthma, and other inflammatory disorders.

References

1 Sheffer AL. Guidelines for the diagnosis and management of asthma. National Heart, Lung, and Blood Institute. National Asthma Education Program. Expert Panel Report. J Allergy Clin Immunol 1991; **88**:425–34.

2 Bittleman DB, Casale TB. Allergic models and cytokines. Am J Respir Crit Care Med 1994; **150**:S72–6.

3 Ball TM, Castro-Rodriguez JA, Griffith KA, Holberg CJ, Martinez FD, Wright AL. Siblings, day-care attendance, and the risk of asthma and wheezing during childhood. N Engl J Med 2000; **343**:538–43.

4 Riedler J, Braun-Fahrlander C, Eder W *et al.* Exposure to farming in early life and development of asthma and allergy: a cross-sectional survey. Lancet 2001; **358**:1129–33.

5 Van Eerdewegh P, Little RD, Dupuis J *et al.* Association of the ADAM33 gene with asthma and bronchial hyperresponsiveness. Nature 2002; **418**:426–30.

6 McIntire JJ, Umetsu SE, Akbari O *et al.* Identification of Tapr (an airway hyperreactivity regulatory locus) and the linked Tim gene family. Nat Immunol 2001; **2**:1109–16.

7 Coffman RL, Seymour BW, Lebman DA *et al.* The role of helper T cell products in mouse B cell differentiation and isotype regulation. Immunol Rev 1988; **102**:5–28.

8 Mosmann TR, Coffman RL. TH1 and TH2 cells: different patterns of lymphokine secretion lead to different functional properties. Annu Rev Immunol 1989; **7**:145–73.

9 Abbas AK, Murphy KM, Sher A. Functional diversity of helper T lymphocytes. Nature 1996; **383**:787–93.

10 Corrigan CJ, Kay AB. CD4 T-lymphocyte activation in acute severe asthma. Relationship to disease severity and atopic status. Am Rev Respir Dis 1990; **141**:970–7.

11 Cembrzynska-Nowak M, Szklarz E, Inglot AD, Teodorczyk-Injeyan JA. Elevated release of tumor necrosis factor-alpha and interferon-gamma by bronchoalveolar leukocytes from patients with bronchial asthma. Am Rev Respir Dis 1993; **147**:291–5.

12 Hansen G, Berry G, DeKruyff RH, Umetsu DT. Allergen-specific Th1 cells fail to counterbalance Th2 cell-induced airway hyperreactivity but cause severe airway inflammation. J Clin Invest 1993; **103**:175–83.

13 Dahl ME, Dabbagh K, Liggitt D, Kim S, Lewis DB. Viral-induced T helper type 1 responses enhance allergic disease by effects on lung dendritic cells. Nat Immunol 2004; **5**:337–43.

14 Kruschinski C, Skripuletz T, Bedoui S, Tschering T, Pabst R, Nassenstein C, Braun A, von Horsten S. CD26 (dipeptidyl-peptidase IV)-dependent recruitment of T cells in a rat asthma model. Clin Exp Immunol 2004; **139**:17–24.

15 Morimoto C, Schlossman SF. The structure and function of CD26 in the T-cell immune response. Immunol Rev 1998; **161**:55–70.

16 Tanaka T, Camerini D, Seed B, Torimoto Y, Dang NH, Kameoka J, Dahlberg HN, Schlossman SF, Morimoto C. Cloning and func-

tional expression of the T cell activation antigen CD26. J Immunol 1992; **149**:481–6.

17 Schrum S, Probst P, Fleischer B, Zipfel PF. Synthesis of the CC-chemokines MIP-1alpha, MIP-1beta, and RANTES is associated with a type 1 immune response. J Immunol 1996; **157**:3598–604.

18 Oravecz T, Pall M, Roderiquez G, Gorrell MD *et al.* Regulation of the receptor specificity and function of the chemokine RANTES (regulated on activation, normal T cell expressed and secreted) by dipeptidyl peptidase IV (CD26)-mediated cleavage. J Exp Med 1997; **186**:1865–72.

19 Ohtsuki T, Hosono O, Kobayashi H, Munakata Y, Souta A, Shioda T, Morimoto C. Negative regulation of the anti-human immunodeficiency virus and chemotactic activity of human stromal cell-derived factor α by CD26/dipeptidyl peptidase IV. FEBS Lett 1998; **431**:236–40.

20 Proost P, Struyf S, Schols D *et al.* Truncation of macrophage-derived chemokine by CD26/ dipeptidyl-peptidase IV beyond its predicted cleavage site affects chemotactic activity and CC chemokine receptor 4 interaction. J Biol Chem 1999; **274**:3988–93.

21 Morimoto C, Torimoto Y, Levinson G, Rudd CE, Schrieber M, Dang NH, Letvin NL, Schlossman SF. 1F7, a novel cell surface molecule, involved in helper function of CD4 cells. J Immunol 1989; **142**:3430–9.

22 Dang NH, Torimoto Y, Deusch K, Schlossman SF, Morimoto C. Comitogenic effect of solid-phase immobilized anti-1F7 on human CD4 T cell activation via CD3 and CD2 pathways. J Immunol 1990; **144**:4092–100.

23 Ishii T, Ohnuma K, Murakami A, Takasawa N, Kobayashi S, Dang NH, Schlossman SF, Morimoto C. CD26-mediated signaling for T cell activation occurs in lipid rafts through its association with CD45RO. Proc Natl Acad Sci USA 2001; **98**:12138–43.

24 Dang NH, Torimoto Y, Schlossman SF, Morimoto C. Human CD4 helper T cell activation. functional involvement of two distinct collagen receptors, 1F7 and VLA integrin family. J Exp Med 1990; **172**:649–52.

25 Tanaka T, Kameoka J, Yaron A, Schlossman SF, Morimoto C. The costimulatory activity of the CD26 antigen requires dipeptidyl peptidase IV enzymatic activity. Proc Natl Acad Sci USA 1993; **90**:4586–90.

26 Eguchi K, Ueki Y, Shimomura C *et al.* Increment in the Ta1+ cells in the peripheral blood and thyroid tissue of patients with Graves' disease. J Immunol 1989; **142**:4233–40.

27 Reinhold D, Bank U, Buhling F, Lendeckel U, Faust J, Neubert K, Ansorge S. Inhibitors of dipeptidyl peptidase IV induce secretion of transforming growth factor-β1 in PWM-stimulated PBMC and T cells. Immunology 1997; **91**:354–60.

28 Willheim M, Ebner C, Baier K *et al.* Cell surface characterization of T lymphocytes and allergen-specific T cell clones: correlation of CD26 expression with T (H1) subsets. J Allergy Clin Immunol 1997; **100**:348–55.

29 Ohnuma K, Munakata Y, Ishii T *et al.* Soluble CD26/dipeptidyl peptidase IV induces T cell proliferation through CD86 up-regulation on APCs. J Immunol 2001; **167**:6745–55.

30 Ohnuma K, Yamochi T, Uchiyama M *et al.* CD26 up-regulates expression of CD86 on antigen-presenting cells by means of caveolin-1. Proc Natl Acad Sci USA 2004; **101**:14186–91.

31 Mizokami A, Eguchi K, Kawakami A *et al.* Increased population of high fluorescence 1F7 (CD26) antigen on T cells in synovial fluid of patients with rheumatoid arthritis. J Rheumatol 1996; **23**:2022–6.

32 Muscat C, Bertotto A, Agea E, Bistoni O *et al.* Expression and functional role of 1F7 (CD26) antigen on peripheral blood and synovial fluid T cells in rheumatoid arthritis patients. Clin Exp Immunol 1994; **98**:252–6.

33 Gerli R, Muscat C, Bertotto A, Bistoni O *et al.* CD26 surface molecule involvement in T cell activationand lymphokine synthesis in rheumatoid and other inflammatory synovitis. Clin Immunol Immunopathol 1996; **80**:31–7.

34 Masuyama J, Berman JS, Cruikshank WW, Morimoto C, Center DM. Evidence for recent as well as long-term activation of T cells migrating through endothelial cell monolayers in vitro. J Immunol 1992; **148**:1367–74.

35 Allen M, Heinzmann A, Noguchi E *et al.* Positional cloning of a novel influencing asthma from chromosome 2q14. Nat Genet 2003; **35**:258–63.

0888-8809/05/$15.00/0
Printed in U.S.A.

Molecular Endocrinology 19(5):1110–1124

doi: 10.1210/me.2004-0264

The Distinct Agonistic Properties of the Phenylpyrazolosteroid Cortivazol Reveal Interdomain Communication within the Glucocorticoid Receptor

Noritada Yoshikawa, Keiko Yamamoto, Noriaki Shimizu, Sachiko Yamada, Chikao Morimoto, and Hirotoshi Tanaka

Division of the Clinical Immunology, the Advanced Clinical Research Center, the Institute of Medical Science, the University of Tokyo, Tokyo 108-8639; and the Institute of Biomaterials and Bioengineering, Tokyo Medical and Dental University, Tokyo 101-0062, Japan

Recent structural analyses of the nuclear receptors establish a paradigm of receptor activation, in which agonist binding induces the ligand binding domain (LBD)/activation function-2 helix to form a charge clamp for coactivator recruitment. However, these analyses have not sufficiently addressed the mechanisms for differential actions of various synthetic steroids in terms of fine tuning of multiple functions of whole receptor molecules. In the present study, we used the glucocorticoid receptor (GR)-specific agonist cortivazol (CVZ) to probe the plasticity and functional modularity of the GR. Structural docking analysis revealed that although CVZ is more bulky than other agonists, it can be accommodated in the ligand binding pocket of the GR by reorientation of several amino acid side chains but without major alterations in the active conformation of the LBD. In this induced fit model, the phenylpyrazole A-ring of CVZ establishes additional contacts with helices 3 and 5 of the LBD that may contribute to a more stable LBD configuration. Structural and functional analysis revealed that CVZ is able to compensate for the deleterious effects of a C-terminal deletion of the LBD in a manner that mimics the stabilizing influence of the F602S point mutation. CVZ-mediated productive recruitment of transcriptional intermediary factor 2 to the C-terminally deleted LBD requires the receptor's own DNA binding domain and is positively influenced by the N-terminal regions of GR or progesterone receptor. These results support a model where ligand-dependent conformational changes in the LBD play a role in GR-mediated gene regulation via modular interaction with the DBD and activation function-1. (*Molecular Endocrinology* 19: 1110–1124, 2005)

GLUCOCORTICOIDS ARE PRODUCED in the adrenal cortex under the strict control of the hypothalamus-pituitary-adrenal axis and exert a variety of biological actions including the regulation of glucose and lipid metabolism, electrolyte balance, and modulation of the immune, cardiovascular, and central nervous system (1, 2). Multiple compounds with glucocorticoid activity including dexamethasone (DEX), prednisolone, and cortivazol (CVZ) are widely used as an antiinflammatory and/or immunosuppressive agents (3). At pharmacological doses, however, patients often suffer from side effects of glucocorticoids, the molecular basis for which have not been fully clarified. Indeed, dissociation of their therapeutic effects and adverse reactions is still one of the most challenging clinical issues to be solved (4, 5).

Glucocorticoids act by the binding to their cognate receptor, the glucocorticoid receptor (GR), the prototypic member of the nuclear receptor superfamily, which also includes the receptors for the mineralocorticoids (MR), estrogens, progestins (PR), and androgens (AR), as well as those for peroxisome proliferators, vitamin D, and thyroid hormones (6, 7). Phylogenetic and sequence analysis indicate that the GR, MR, PR, and AR form a subfamily of oxosteroid receptors (6, 7). Like most nuclear receptors, the GR is a modular protein that is organized into three major domains: an N-terminal regulatory domain harboring a strong transcriptional activation function (AF)-1, a central DNA binding domain (DBD), and a C-terminal ligand binding domain (LBD) (6, 8). The LBD harbors a second AF-2 directly regulated by ligands. Agonist binding to the LBD induces the reorientation of a critical α-helix (AF-2 helix) and the formation of a binding pocket for a family of coactivator proteins that play

First Published Online January 27, 2005

Abbreviations: AF, Activation function; AR, androgen receptor; CVZ, cortivazol; DBD, DNA binding domain; DEX, dexamethasone; GFP, green fluorescent protein; GR, glucocorticoid receptor; GRE, glucocorticoid response element; hsp90, heat shock protein 90; LBD, ligand binding domain; MR, mineralocorticoid receptor; NF-κB, nuclear factor-κ B; NLS, nuclear localization signal; PR, progesterone receptor; SDS, sodium dodecyl sulfate; TIF, transcriptional intermediary factor.

***Molecular Endocrinology* is published monthly by The Endocrine Society (http://www.endo-society.org), the foremost professional society serving the endocrine community.**

essential roles in transactivation (9, 10). Among nuclear receptors, the AF-2 pocket is highly conserved, whereas the molecular size and amino acid composition of AF-1 is much more diverse (6, 9). In the absence of ligand, the GR is retained in the cytoplasm in association with chaperone proteins such as heat shock protein 90 (hsp90) (11, 12). Hormone binding initiates the release of the chaperone proteins and translocation of the receptor into the nucleus where GR binds to DNA promoter elements termed glucocorticoid response element (GRE) from which it can either activate or repress transcription depending on the context of the target promoter (6, 8). In addition, the GR also interacts with other transcription factors such as nuclear factor-κB (NF-κB) to repress their transcriptional activities. This GR-mediated repression has been postulated to be one of the major mechanisms for the therapeutic antiinflammatory and immunosuppressive activities of glucocorticoids (13, 14).

Recent crystallographic analyses of the nuclear receptors have clarified the relationship between receptor structure and function and established a paradigm of receptor activation. The GR LBD, similar to other nuclear receptor LBDs, is composed of α-helices and β-strands folded into a three-layer helical sandwich. The ligand binding pocket is composed of residues from helices 3, 4, 5, 6, 7, 10, and the AF-2 helix as well as residues from β-strands between helices 5 and 6. Following AF-2 helix is an extended strand that forms a conserved β-sheet with a β-strand between helices 8 and 9. This C-terminal β-strand also appears to play an important role in receptor activation by stabilizing AF-2 helix in an active conformation (15, 16). Many AF-2 coactivators for the GR have been identified to date, including steroid receptor coactivator-1, transcriptional intermediary factor (TIF) 2/GR-interacting protein-1 and cAMP response element binding protein-binding protein/p300 (17–21). These coactivators directly associate with the GR LBD via their LXXLL motif. For example, the LLRYLL sequence in the TIF2 forms a two-turn α-helix that orients the hydrophobic leucine side chains into a groove formed in part by the AF-2 helix and residues from helices 3, 3′, 4, and 5. The N- and C-terminal ends of the coactivator helix are clamped by Glu-755 from the AF-2 helix and Lys-579 in helix 3, respectively (15). Mutations that disrupt either the first (Glu-755) or the second (Arg-585 and Asp-590) charge clamp dramatically reduce activation mediated by the GR LBD, demonstrating that they are critical for transactivation function of the GR (15). On the other hand, AF-1 coactivators have only recently been described. For example, basal transcription factors including TBP and TFIID have been shown to associate with the AF-1 of GR (22, 23). TSG101 and DRIP150 have also been reported to interact with GR AF-1 and regulate GR function in a reciprocal manner; GR transcriptional activities are repressed by TSG101 but enhanced by DRIP150 (24). These cofactors are shown to interact with distinct regions of AF-1 (22–24). Although we now have at hand a large number of regulatory proteins that interact directly or indirectly with the various modular domains of nuclear receptors, how ligands differentially regulate the functional interplay between them remains poorly understood.

The phenylpyrazologlucocorticoid CVZ is a unique synthetic glucocorticoid agonist with complex binding properties and is more potent than DEX (25). We previously demonstrated that CVZ selectively binds to the GR but not to the MR and, based on two criteria, we proposed that the functional interaction of CVZ with the GR LBD is different from that of DEX. Firstly, deletion of the last 12 amino acids of GR severely compromises DEX but not CVZ binding and secondly, the point mutant L753F, in which Leu-753 in AF-2 is substituted to Phe, can efficiently recruit TIF2 to the LBD when bound to CVZ but not when bound to DEX (26). These results prompted us to propose that occupancy of the GR LBD by CVZ might lead to a more stable active conformation that can tolerate the disrupting effects of LBD mutations and may have unique effects on the structure and function of the whole GR molecule. In the present study, we explore the distinct properties of CVZ-bound GR by modeling its structure, analyzing the influence of both destabilizing and stabilizing LBD mutations, and probing the role played by other receptor domains. We provide evidence that the CVZ-specific LBD conformation allows efficient TIF2 recruitment to the receptor at least in part through intrareceptor communication between the LBD and DBD, as well as through collaboration with N-terminal sequences.

RESULTS

Docking Model of CVZ-Bound GR LBD

Because we and others showed that CVZ-bound GR has distinct functional characteristics when compared with DEX-bound GR (see introductory section), we first examined whether CVZ could be accommodated into the classical ligand binding pocket of the GR LBD or whether a distinct binding mode must be invoked. For this purpose, we modeled the three-dimensional structure of CVZ-bound GR using the coordinates of the crystal structure between the F602S mutant LBD and DEX (15). In brief, we docked CVZ *in silico* into the ligand binding pocket of the GR LBD by superimposing its steroid backbone with that of DEX. The calculated volume of DEX and CVZ is 386 Å^3 and 541 Å^3, respectively, reflecting that CVZ has a bulky phenylpyrazole ring attached to the A-ring of steroid backbone as well as a C21-acetoxyl group at the D-ring (Fig. 1A). The estimated volume of the ligand binding pocket of the GR LBD is 600 Å^3, which appears to be large enough for binding either ligand. Energy minimization of the CVZ/GR LBD complex suggested that favorable configurations between GR and CVZ could be reached by the induced fit mechanism. The resultant model for CVZ-GR LBD is shown in Fig. 1B. CVZ,

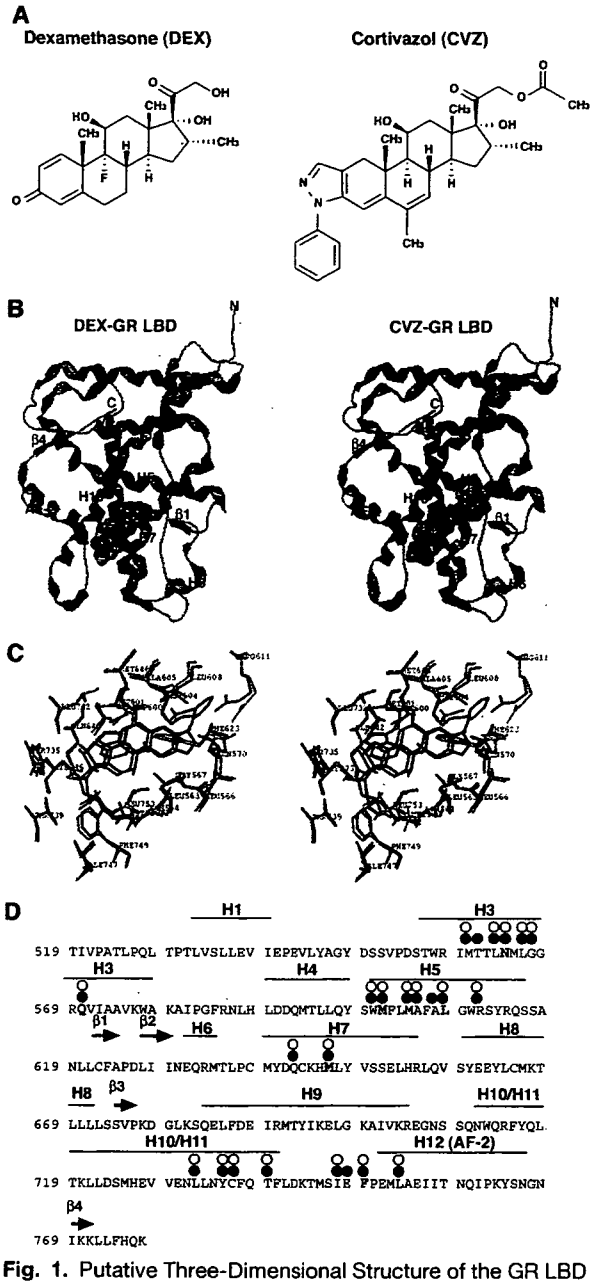

Fig. 1. Putative Three-Dimensional Structure of the GR LBD Docked with DEX and CVZ

A, Structure of DEX and CVZ. B, Overall arrangement of DEX- and CVZ-bound GR LBD. Ribbons represent α-helices and β-strands, and tubes represent loops of the protein. The GR-LBD docked with DEX or CVZ is depicted with space fill model. C, Ligand binding pocket of GR-DEX complex superimposed with that of GR-CVZ one (StereoView 20/20, 3D Experience, Hertfordshire, UK). Structures are drawn with stick model. Amino acid residues of GR-DEX and GR-CVZ complex are drawn by *green* and *orange sticks*, respectively. DEX and CVZ are depicted with *blue* and *red*, respectively. D, Amino acid sequence and secondary structure of the GR LBD. Amino acid sequence of the GR LBD and the location of α-helices (H1 to H12, *bold bars*) and β-strands (β1 to β4, *arrows*) are schematically illustrated. *Number* depicts the position of amino acids. *Open* and *filled circles* indicate the GR residues closer than 4.5 Å to DEX and CVZ, respectively.

as well as DEX, is completely enclosed within the bottom half of the GR LBD and spatial position of the α-helices and β-strands of the CVZ-bound GR LBD is almost identical with that of DEX-bound one, including the orientation of helix 12. One or more hydrophobic residues within the GR protein contact nearly every atom of the steroid core of DEX and CVZ (Fig. 1C). In addition, the model allows for all of the hydrophilic groups of CVZ to form hydrogen bonds with the protein, which is what is observed in the DEX structure (Fig. 1C). A similar and extensive hydrogen bond network between GR and either DEX or CVZ is likely to contribute to their high affinity binding. Moreover, both ligands make direct contacts with AF-2 helix at Leu-753 and the loop preceding AF-2 helix at Ile-747 and Phe-749 (Fig. 1C). These interactions are likely to stabilize the AF-2 helix in the active conformation in CVZ-bound LBD and are consistent with the strong agonistic activities of CVZ.

Given the extra volume of CVZ, several differences between the DEX-bound GR LBD complex and our model are also evident. To accommodate the bulky phenylpyrazole ring and 21-acetoxyl group of CVZ, the position of the side chain of Arg-611 is shifted outward of the ligand binding pocket and side chain conformations of Asn-564, Gln-570, Met-604, Leu-608, Met-646, and Phe-749 are altered, resulting in distinct hydrogen bond network (Fig. 1, C and D). Notably, all of these amino acids except for Phe-749 originate from helices 3 and 5. Taken together, the modeling suggests that CVZ might stably bind with the GR and elicit its distinct effects on GR function via minor local alteration in the conformation of these helices.

Discrimination of Glucocorticoid Ligands by GR Variants with Destabilizing and Stabilizing Mutations

We have previously shown that deletion of the last 12 amino acids severely compromises DEX binding and DEX-dependent activity but CVZ binding activity is preserved (26). In contrast to this deleterious deletion, the Phe-602 to Ser substitution in the GR LBD has been shown to stabilize the binding of various ligands and was instrumental in the successful crystallization of the GR LBD (15, 16, 27). We therefore hypothesized that this substitution might counteract the deleterious effects of C-terminal deletion and restore DEX function. We thus introduced this mutation in the context of the C-terminally deleted GR-(1–765) (resultant mutant is GR-(1–765)/F602S, Fig. 2A). These mutants should be useful tools to contrast the characteristics of the interaction between CVZ and DEX with the GR.

Initially, we characterized these mutants biochemically. Because hsp90 is essential for ligand binding, we addressed whether these mutant GR could bind hsp90 *in situ* (Fig. 2B). To this end, COS7 cells were transfected with expression plasmids for the wild-type and mutant GR forms, and cellular lysates were prepared in the absence of ligand. Protein expression of

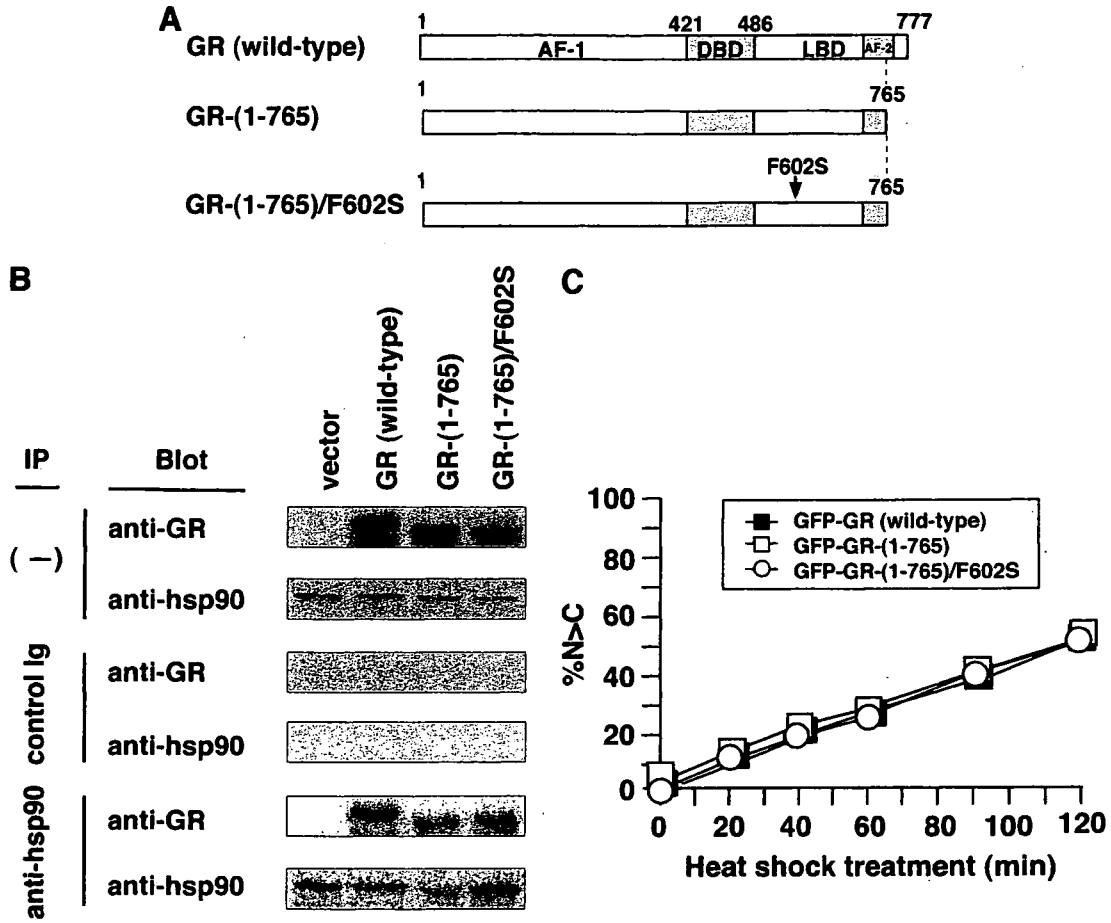

Fig. 2. Association of hsp90 with the GR LBD Is Not Affected by Either C-Terminal Truncation or F602S Substitution in the GR

A, Schematic illustration of the wild-type and C-terminally truncated human GR. The number depicts the position of amino acid. GR-(1–765) lacks 12 amino acids from the C-terminal end of the LBD. GR-(1–765)/F602S contains the additional amino acid substitution from Phe-602 to Ser (F602S, *arrowhead*) in the context of GR-(1–765). B, Association of hsp90 with the GR and its C-terminally truncated mutants. After transfection of pCMX, pCMX-GR, pCMX-GR-(1–765), or pCMX-GR-(1–765)/F602S into COS7 cells, the cells were cultured in the absence of ligand for 24 h and whole cell extracts were prepared and coimmunoprecipitated with hsp90-specific antibodies or control mouse Ig. Whole cell extracts or immunoprecipitated proteins were run on 6% SDS-polyacrylamide gels. Western immunoblotting was performed using anti-GR or anti-hsp90 antibodies as described in *Materials and Methods*. IP, Antibodies for immunoprecipitation. Blot, antibodies for Western immunoblotting. C, Subcellular localization of the GFP-tagged wild-type and C-terminal truncated GR after heat shock. COS7 cells expressing either GFP-tagged protein GFP-GR (wild type), GFP-GR-(1–765), or GFP-GR-(1–765)/F602S were cultured in a humidified 5% CO_2 atmosphere at 43 C, and subcellular localization of the proteins was analyzed as described in *Materials and Methods*. Results represent the percentage of nuclear-dominant fluorescent cells (%*N* > C). Experiments were repeated three times with almost identical results, and representative graph is shown.

the wild-type GR and its mutants was comparable (Fig. 2B). As shown in Fig. 2B, the wild-type GR and its mutant forms can be immunoprecipitated with anti-hsp90 antibodies but not control Ig. The functional significance of this association was confirmed in heat-shock experiment. As seen in Fig. 2C, treatment of transfected cells at 43 C for 2 h promoted nuclear translocation of green fluorescent protein (GFP)-fused GR and its mutants. We concluded that neither the C-terminal deletion nor F602S substitution within GR-(1–765) grossly affected the association of hsp90 with the GR LBD in the absence of ligand.

Next, we performed protease digestion experiments because this assay, albeit indirectly, can simultaneously assess ligand binding and the subsequent conformational alteration of the receptor (28, 29). For this purpose, GR proteins were translated *in vitro* in the presence of [^{35}S]Met and incubated in the presence or absence of DEX or CVZ, followed by digestion with various concentrations of trypsin. As shown in Fig. 3A, in the absence of ligand, wild-type and mutant GRs were completely processed at a trypsin concentration of 5 μg/ml. In the presence of 10 μM DEX or CVZ, however, the wild-type GR was protected from the enzymatic digestion and stable 30- and 27-kDa fragments were produced, indicating that ligand binding altered and stabilized the LBD conformation into trypsin-resistant form. In

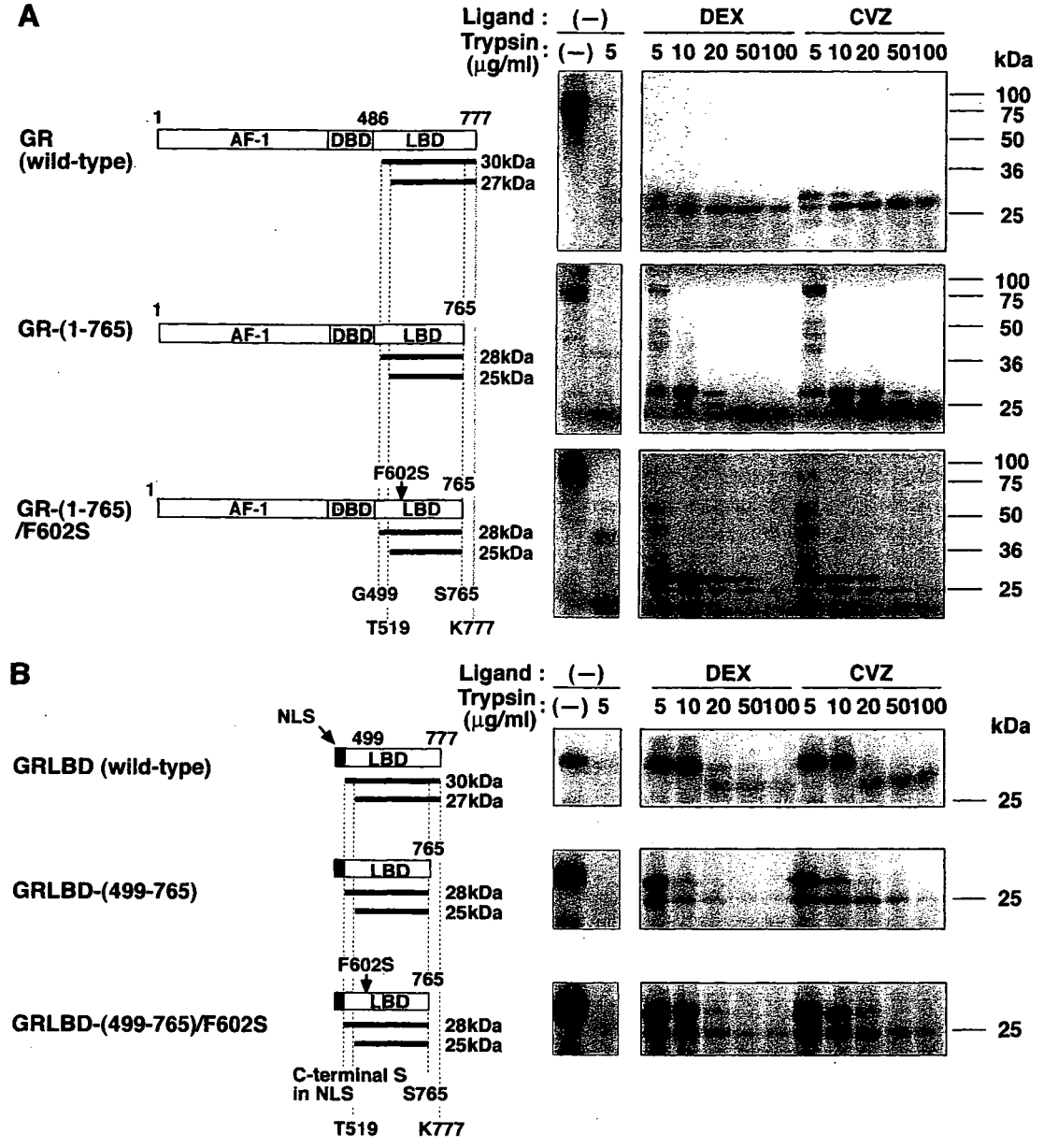

Fig. 3. Effects of DEX and CVZ on Proteolytic Digestion of *in Vitro*-Translated Wild-Type and C-Terminal Truncated GR

Schematic illustration of the wild-type GR, GR-(1–765), and GR-(1–765)/F602S (A), and NLS-fused GR LBD, GRLBD-(499–765), and GRLBD-(499–765)/F602S (B) are shown in the *left*. The predicted trypsin-resistant fragments are depicted as *bold lines* with their calculated molecular weights (45, 61). Representative results from trypsin digestion assays are presented in the *right*. In brief, *in vitro*-synthesized [^{35}S]GR and its mutants (A), or [^{35}S]GRLBD and its mutants (B) was incubated with either vehicle or 10 μM of DEX or CVZ for 30 min at 20 C; then the indicated concentrations of trypsin were added and digestion was preceded for 10 min at 20 C as described in *Materials and Methods*. Samples were denatured and separated on 12% SDS-polyacrylamide gels. Gels were processed as described in *Materials and Methods* for visualization and representative results are shown.

contrast to the wild-type GR, the C-terminally deleted receptor discriminated between the two ligands because CVZ was able to protect the LBD from digestion with 50 and 100 μg/ml of trypsin (generating 25- and 28-kDa fragments), whereas DEX was substantially less effective. Consistent with our hypothesis, addition of the F602S mutation within the context of the C-terminal deletion partially restored the ability of DEX to protect against 50 and 100 μg/ml of trypsin. This suggests that this amino acid substitution enabled DEX to more efficiently bind and stabilize the deleted LBD just as CVZ can do in the absence of the point mutation (Fig. 3A).

These results were further supported in separate experiments using constructs expressing a fusion protein between the simian virus 40 nuclear localization signal (NLS) and the GR LBD alone (Fig. 3B). In the absence of ligands, *in vitro*-translated wild-type and

mutant LBDs were completely digested (Fig. 3B). In the presence of DEX or CVZ, however, trypsin treatment of the wild-type LBD generated stable 30- and 27-kDa fragments (Fig. 3B). As in the case of the full-length GR, the C-terminally deleted LBD [LBD-(499–765)] was resistant to trypsin in the presence of CVZ but not DEX. Moreover, the F602S substitution enabled DEX to protect this LBD. Taken together, these results indicate that CVZ-bound GR mimics the more stable conformation achieved by DEX in the presence of the F602S point mutation.

Distinct Effects of DEX and CVZ on the Function of C-Terminally Truncated GR

We next studied the effect of treatment with DEX and CVZ on nuclear translocation of GR and its mutants using GFP-tagged forms. The mutations did not alter the behavior of the receptor in the absence of ligands because GFP-tagged GR and its mutants are all localized in the cytoplasm. In the case of wild-type GFP-GR, both DEX and CVZ promoted efficient nuclear translocation (Fig. 4A). In contrast, whereas CVZ was able to induce nuclear translocation of GFP-GR-(1–765), DEX failed to do so (Fig. 4A). Notably, introduction of the F602S mutation restored the ability of DEX to induce the translocation of the C-terminally deleted receptor and eliminated the difference between the ligands (Fig. 4A). These results again suggested that the F602S substitution appears to stabilize DEX-binding to GR-(1–765).

To assess the effect of DEX and CVZ on the transactivation function of wild-type and mutant GRs, we used a GRE-driven luciferase reporter plasmid in COS7 cells. As previously reported, DEX and CVZ induced GRE-dependent transactivation by the wild-type GR, whereas reporter gene activation by GR-(1–765) was only observed for CVZ (Fig. 4B). Surprisingly, although DEX and CVZ were able to induce nuclear translocation and DNA binding activities of GR-(1–765)/F602S (Fig. 4A and data not shown), DEX scarcely induced transactivation even at high concentrations, whereas CVZ elicited gene activation in a concentration-dependent manner (Fig. 4B). Because it has been shown that ligand binding affects stability of the GR (30), we examined GR protein levels after treatment with DEX or CVZ. As previously reported, treatment with DEX or CVZ decreased the protein levels of the GFP-fused full-length GR (Fig. 4C). In clear contrast, DEX treatment did not lead to reduced protein levels of either GFP-GR-(1–765) or GFP-GR-(1–765)/F602S (Fig. 4C). Moreover, CVZ showed only marginal decrease in the protein levels of these mutant GRs (Fig. 4C). These results reveal a role for the C-terminal 12 amino acids in down-regulation of the receptor but indicate that the differential effects of DEX and CVZ on GR-mediated reporter gene activation is not simply due to ligand-induced decrease of GR protein stability. The striking difference in transactivation between DEX- and CVZ-bound GR mutants coupled with our structural prediction that CVZ-bound LBD might lead to only minor conformational alteration in the LBD when compared with DEX suggests that such subtle conformational changes might affect ligand-dependent cofactor recruitment to the receptor, especially because it has already been reported that in addition to AF-2, N-terminal segments of the LBD are important for stable interaction with coactivators (15, 31). We therefore examined the effect of exogenous expression of TIF2 on the ability of the various GR mutants to induce transcription in response to DEX and CVZ. Overexpression of TIF2-enhanced CVZ-induced transactivation by the wild-type GR as well as GR-(1–765) and GR-(1–765)/F602S (Fig. 5B). On the other hand, TIF2 only marginally rescued DEX-dependent transactivation by either mutant (Fig. 5B).

To test the possibility that TIF2 recruitment is influenced by sequences within the N-terminal domain of the receptor, we exchanged this region of the GR and its mutants with those of the MR and PR (Fig. 5A). Deletion of AF-1 (GRΔAF-1) resulted in a 60% decrease in activity, which was still enhanced by TIF2. As previously reported (32), replacement of the N-terminal region of the GR with that of the MR did not significantly enhance activity compared with GRΔAF-1. Enhancement of CVZ-mediated transactivation by TIF2 was observed in M/GG/765 and M/GG/765/F602S as seen in GRΔAF-1 and M/GG. The N-terminal region of PR functionally substituted for that of GR and TIF2 enhancement is observed for both P/GG/765 and P/GG/765/F602S (Fig. 5B). These results argue that although AF-1 cooperates with AF-2, it does not play a critical role in CVZ-mediated recruitment of TIF2 to the receptor.

To confirm the effects of these ligands on the interaction between the GR and TIF2 *in situ*, we performed immunofluorescence colocalization assays in which GFP-GR and TIF2 were coexpressed. As previously reported (26), wild-type GR displace a speckled localization in the nucleus in the presence of TIF2 (Fig. 5C and data not shown). Consistent with the transactivation data, CVZ induced this speckled pattern for both GR-(1–765) and GR-(1–765)/F602S, whereas DEX treatment failed to translocate GR-(1–765) and resulted in a diffuse nuclear localization of GR-(1–765)/F602S (Fig. 5C). Thus, although DEX-bound GR-(1–765)/F602S accumulates in the nucleus, it does not appear to form transcriptionally productive complex with TIF2.

Ligand-Dependent Scenario for Communication between DBD and the LBD

To further delineate the receptor domains involved in the differential properties of DEX- *vs.* CVZ-bound GR, we next examined the ability of CVZ to counteract the deleterious effects of the C-terminal deletion and support the recruitment of TIF2 in the context of the GR LBD alone. To test this, we constructed plasmids for the expression of GAL4 DBD-GR LBD fusion proteins

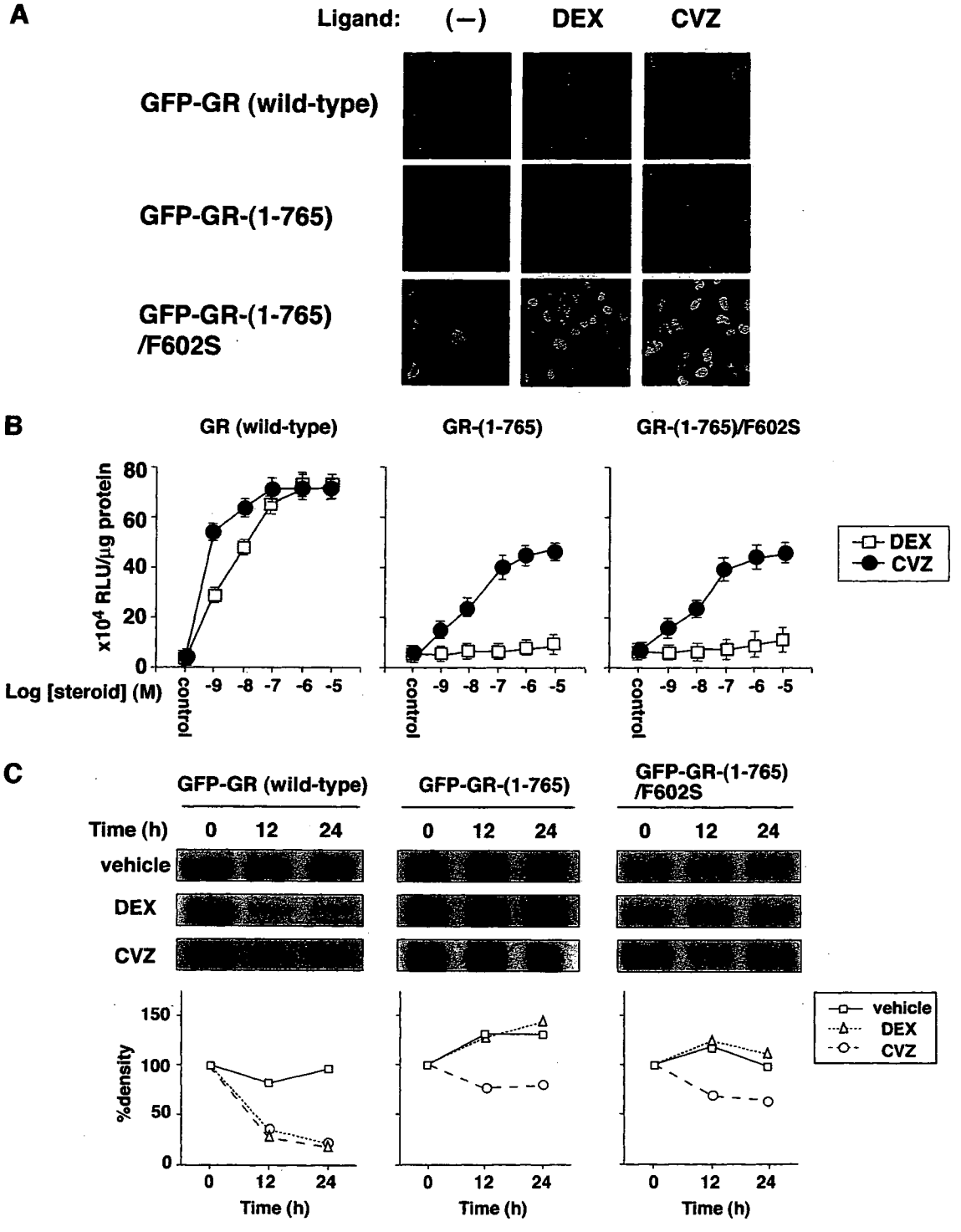

Fig. 4. C-Terminal Truncation of the LBD with F602S Substitution Unveils Differential Effects of DEX and CVZ on Transactivation Function of the GR

A, Effects of ligands on subcellular localization of the GR and its C-terminally truncated mutants. GFP-tagged wild-type GR, GR-(1–765), and GR-(1–765)/F602S were transiently expressed in COS7 cells and the cells were cultured in the presence or absence of 1 μM of DEX or CVZ for 2 h, then digital images were taken as described in *Materials and Methods* and representative results are shown. B, Differential effects of DEX and CVZ on GRE-driven reporter gene expression. COS7 cells were cotransfected with 2 μg of GRE-driven reporter plasmid pGRE-LUC and 100 ng of expression plasmids for either wild-type GR, GR-(1–765), or GR-(1–765)/F602S, and cultured in the absence or presence of the indicated concentrations of DEX or CVZ for 24 h. Cellular luciferase activities were measured as described in *Materials and Methods*. Experiments were performed in triplicate and results are expressed as relative light units (RLU) per microgram of protein in the extract, and the means ± SD are shown. C, Effects of DEX and CVZ on receptor protein levels. COS7 cells were transiently transfected with expression plasmids for GFP-tagged

[GAL4-GRLBD, GAL4-GRLBD-(489–765), and GAL4-GRLBD-(489–765)/F602S; see Fig. 6A], and tested them in a mammalian one-hybrid assay using GAL4-responsive reporter plasmid in COS7 cells. Nuclear translocation assays paralleled the observations using the intact GR and confirmed that CVZ could achieve nuclear entry of all the chimeric proteins, whereas DEX induced the translocation of only GAL4-GRLBD and GAL4-GRLBD-(489–765)/F602S (Fig. 6A). The GAL4-GRLBD chimera activated the reporter gene in response to both DEX and CVZ and heterologous expression of TIF2 enhanced this response, indicating that binding of either ligand facilitated the recruitment of TIF2 to the LBD alone. Deletion of the last 12 amino acids of the LBD severely compromised CVZ as well as DEX induction even in the presence of TIF2 or after combining it with the F602S substitution (Fig. 6B). Both ligands induced substantial down-regulation of the wild-type LBD fusion chimera, whereas the levels of GAL4-GRLBD-(489–765) and GAL4-GRLBD-(489–765)/F602S were mildly affected or unchanged (Fig. 6C). These results indicate that the deleterious effects of the C-terminal truncation cannot be counteracted by CVZ binding or the F602S substitution in the context of the LBD alone and suggest that additional domains are required.

To examine the involvement of the GR DBD, we carried out parallel one-hybrid assays in the context of N-terminally deleted GRΔAF-1 construct where the LBD is recruited to the promoter through the GR's own DBD. As in the case of the GAL4 fusions, CVZ could achieve nuclear entry of all three mutant GR forms, whereas DEX could do so only for GRΔAF-1 and GRΔAF-1/765/F602S (Fig. 6A). In clear contrast to the GAL4 fusion chimeras, CVZ was able to support transactivation after deletion of the last 12 amino acids and TIF2-mediated enhancement was preserved (Fig. 6B). Because the behavior of these N-terminally deleted forms resembled that of the full-length receptor (including the ligand-induced changes in protein level; see Fig. 6C), the results indicate that the DBD of GR is sufficient to support the ability of CVZ to counteract the deleterious effects of the C-terminal deletion and that productive recruitment of TIF2 in this context likely involves a ligand-based functional communication between the LBD and the DBD.

The Functional Differences between CVZ and DEX Are Also Evident during GR Transrepression of NF-κB

To examine whether the induced structural change of the LBD upon CVZ binding affects other receptor functions, we tested the ability of both DEX and CVZ to support GR mediated transrepression of NF-κB-stimulated transcription. Although the mechanism of NF-κB repression by the GR remains to be fully defined, it is known that the p65 subunit of NF-κB physically interact with the GR DBD (33–37). Wild-type GR suppressed NF-κB-dependent transcription in response to both DEX and CVZ (Fig. 7). Deletion of the last 12 amino acids again revealed a marked difference between ligands because CVZ-mediated repression was preserved, whereas the DEX response was essentially abrogated. As in the case of activation, inclusion of the F602S substitution did not restore DEX-mediated inhibition (Fig. 7). These results suggest that CVZ differentially modulates receptor function not only in transactivation but also in transrepression, likely through the establishment of a distinct LBD conformation and functional interaction with the DBD.

DISCUSSION

In the present study, we have explored the mode of binding of the unique glucocorticoid agonist CVZ and have taken advantage of C-terminally deleted GR variants to unveil otherwise hidden differences between CVZ and the prototypic agonist DEX. Ligand binding is believed to give the receptor a cue for activation by the adoption of a conformation that is conducive to interaction with coactivator proteins (38). Data from multiple members of this family indicate that the chemical structure of individual agonists can produce distinct conformations of the LBD with unique regulatory properties (9, 39). Given bulky phenylpyrazole substituent at the A-ring of CVZ, it is thus reasonable to hypothesize that CVZ-bound GR is likely to have a distinct structure when compared with the DEX-bound one. According to our modeling data, CVZ could fit in the ligand binding pocket through an induced fit mechanism (Fig. 1). The additional volume contributed by the phenylpyrazole ring of CVZ provides additional contacts with the protein and can be accommodated through minor alterations in the receptor structure involving the reorientation of amino acid side chains emerging mainly from helices 3 and 5. These alterations may result in the generation of a more stable bound conformation and distinct functional surfaces. Although it is obvious that the direct determination of the structure of CVZ-bound LBD is required to determine the actual mode of binding, data from existing structures are compatible with the model. In the case of the liver X receptor β, the structure of the LBD is

wild-type GR, GR-(1–765), or GR-(1–765)/F602S. The cells were further cultured and treated with vehicle or 1 μM of DEX or CVZ for 0, 12, or 24 h. Whole cell extracts were prepared and 10 μg of protein was separated by SDS-PAGE. Expression levels of each protein were analyzed by Western immunoblotting using anti-GFP antibodies as described in *Materials and Methods*. Data were quantitated and expressed as percentage of density, which was given relative to the density obtained from the cells treated with each ligand for 0 h as described in *Materials and Methods*. Experiments were repeated three times with almost identical results, and representative results are shown.